Accuracy of Arterial Blood Pressure Waveform Measurement via Catheter Manometer Systems in Neonatal Intensive Care

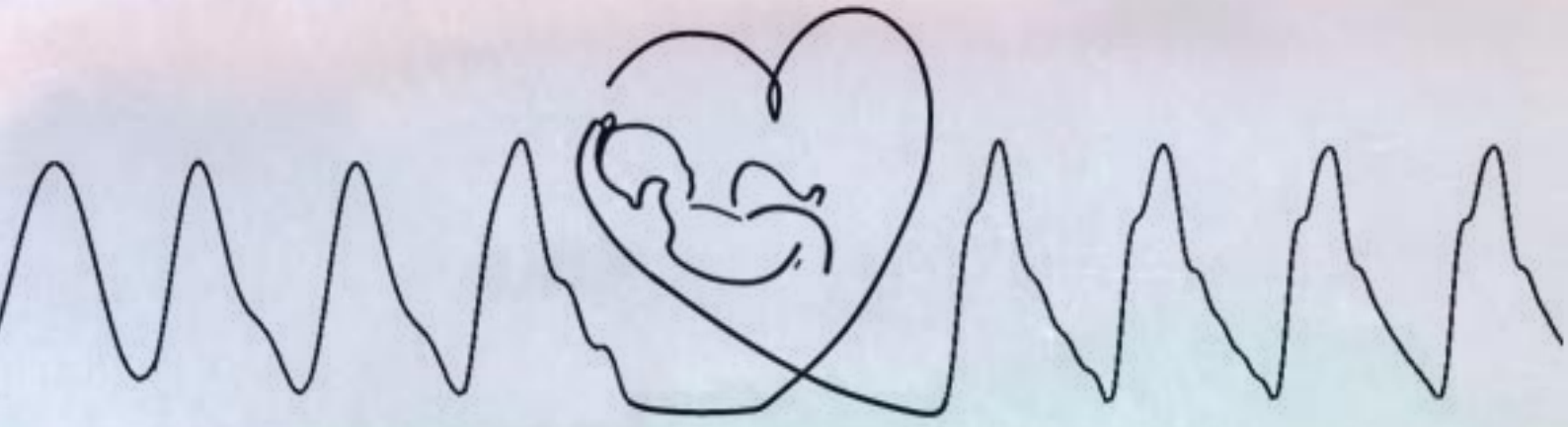

Nienke A. Timmermans

UNIVERSITY OF TWENTE.

Amalia Children's Hospital
Radboudumc

Master Thesis

Technical Medicine – Medical Sensing and Stimulation

Accuracy of Arterial Blood Pressure Waveform Measurement via Catheter Manometer Systems in Neonatal Intensive Care

Nienke Adinda Timmermans

Publication: March 23rd, 2023

Colloquium: April 20th, 2023

Graduation Committee

Chair and Technical supervisor	Prof.dr. H.J. Zwart[1]
Medical supervisor	Prof.dr. W.P. de Boode[2]
Process supervisor	Drs. R.M. Krol[3]
External member	M.M.L.H. Verhulst, MSc[4,5]
Extra member	Dr.ir. B.E. Westerhof[2]

[1] Department of Applied Mathematics, University of Twente
[2] Department of Neonatology, Radboudumc Amalia Children's Hospital
[3] Department of Technical Medicine, University of Twente
[4] Department of Clinical Neurophysiology, Rijnstate Hospital
[5] Clinical Neurophysiology Group, University of Twente

Dankwoord

Het afgelopen jaar heb ik met veel plezier gewerkt aan deze thesis. Ik wil graag iedereen bedanken die daaraan heeft bijgedragen. Willem, dankjewel voor je enthousiasme en betrokkenheid bij het onderzoek als mijn medisch begeleider. Je maakte altijd tijd voor onze wekelijkse meetings en hielp me om de grote lijnen in mijn onderzoek te blijven zien. Hans, bedankt dat je mijn technisch begeleider wilde zijn bij deze voor jou nog nieuwe onderzoekslijn. Jouw kritische vragen hebben me geholpen om mijn onderzoek te verbeteren. Berend, bedankt dat je betrokken wilde blijven bij dit onderzoek als mijn extra begeleider en voor je enthousiasme en uitgebreide feedback op mijn thesis. Ruby, dankjewel voor het zijn van mijn procesbegeleider en de hulp bij het verkrijgen van waardevolle inzichten in mezelf. Als laatste van mijn afstudeercommissie wil ik graag Marlous bedanken voor het zijn van mijn buitenlid.
Daarnaast wil ik graag Lotte bedanken voor al haar geleverde werk en uitleg daarvan, zodat ik daarop kon voortbouwen. Ook wil ik Tim bedanken voor zijn hulp bij het verkrijgen van de data en voor de interessante discussies die we hadden op onze gezamenlijke werkplek. Verder wil ik graag alle neonatale intensive care verpleegkundigen, Wouter en Theo bedanken voor hun hulp bij de metingen die ik heb gedaan. Lieke, Kimmia, Maureen en Carmen, dank jullie wel voor de gezelligheid op de werkplek en de nieuwe ideeën die jullie me gaven voor mijn onderzoek. Josee, Maranda en Jorn, bedankt voor de fijne en gezellige intervisies het afgelopen jaar.
Tenslotte wil ik graag mijn familie en vrienden bedanken voor hun steun bij en interesse in wat ik het afgelopen jaar heb gedaan. Iris, Hille, Fenna en Eva, ik keek altijd uit naar de momenten waarop ik weer met jullie kon bijkletsen. Maarten, dankjewel voor de afleiding die je me bood om niet te veel met mijn onderzoek bezig te zijn, maar ook voor je hulp om bepaalde dingen nog net wat beter te begrijpen. Papa en mama, dank jullie wel dat jullie het mogelijk maakten voor mij om te gaan studeren en jullie onvoorwaardelijke steun bij alles wat ik graag wilde en nog wil gaan doen.

Nienke Timmermans

Nijmegen, maart 2023

Abstract

Background: Advanced analysis of the arterial blood pressure waveform (ABPW), as part of comprehensive hemodynamic monitoring in critically ill neonates, requires an accurate measurement method. Measuring blood pressure with a liquid-filled catheter manometer system (CMS) is currently considered the gold standard in neonates. However, the measured ABPW may be distorted by an inadequate dynamic response (DR) of the CMS. Although it is generally understood how an inadequate DR can affect the measured ABPW in adults, the DR characteristics of the CMS currently used in neonatal intensive care and their effect on the neonatal ABPW remain unknown.

Aim: The primary aim of this study is to evaluate the accuracy of the ABPW measured in neonatal intensive care based on DR characteristics of liquid-filled CMS. To improve the accuracy of the measured ABPW, the secondary aim is to provide the initial validation of a reconstruction method for ABPW in case of inadequate DR.

Methods: First, the flush pulse method for assessing the DR characteristics of neonatal CMS was validated in-vitro. Subsequently, this method was applied to assess the in-vivo DR characteristics of CMS at the neonatal intensive care unit. Computer simulations were performed to quantify the effect of the total monitoring chain, composed of a CMS and monitor low pass filter, on several neonatal ABPW parameters. Lastly, a measurement-specific reconstruction method for distorted ABPW was proposed and initially validated.

Results: DR characteristics were assessed in 18 patients with 20 arterial lines in total. Based on these measurements, computer simulations of the CMS and monitor low pass filter showed that the errors in pulse and dicrotic notch pressures, maximal slope of the systolic upstroke and systolic area under the curve of a neonatal ABPW could exceed 10%. Furthermore, considerable variation in DR characteristics across and within individual arterial lines was found. Initial validation of the proposed reconstruction method for distorted ABPW showed that this method is not yet adequate for clinical practice.

Conclusion: Accuracy of the ABPW measured in critically ill neonates can be considerably affected by the DR of CMS in combination with the monitor low pass filter. Until the accuracy of ABPW measurement is improved or a valid reconstruction method exists, it is not recommended to investigate or implement advanced ABPW analysis techniques in neonatal intensive care.

Keywords: Arterial blood pressure waveform, measurement accuracy, catheter manometer system, dynamic response, neonatal intensive care

List of Abbreviations and Symbols

ABPW	arterial blood pressure waveform
AUC	area under the curve
CMS	catheter manometer system
CO	cardiac output
DNI	dicrotic notch index
DR	dynamic response
F	French (French gauge, indicating the size of umbilical catheters)
FO	foramen ovale
G	Gauge (Birmingham gauge, indicating the size of intravenous cannulas)
IQR	interquartile range
LV	left ventricular
MTC	manometer tipped catheter
NICU	neonatal intensive care unit
N/O	no oscillation
NPE	neonatologist performed echocardiography
PBF	pulmonary blood flow
PDA	patent ductus arteriosus
PP	pulse pressure
PRAM	pressure recording analytical method
PVR	pulmonary vascular resistance
RMSE	root mean square error
ROSE	Resonance OverShoot Eliminator
SBF	systemic blood flow
SV	stroke volume
SVR	systemic vascular resistance

C_d	sensor diaphragm compliance
$\mathrm{d}P/\mathrm{d}t$	slope of the systolic upstroke
ζ	damping coefficient
f_c	cut-off frequency in Hz
f_n	natural frequency in Hz
H	transfer function
η	fluid viscosity
I	output signal
j	imaginary unit
K	elastance
L	catheter length
L_c	catheter liquid inertia
O	output signal
P	pressure
ρ	fluid density
Q	flow
r	catheter radius
R_c	catheter liquid resistance
s	Laplace operator
V	volume
ω_c	cut-off frequency in rad/s
ω_n	natural frequency in rad/s

Table of Contents

Dankwoord iii
Abstract iv
List of Abbreviations and Symbols v
1 Introduction 1
1.1 Aim and Objectives 2
1.2 Thesis Outline 2
2 Background 3
2.1 Developmental Cardiovascular Physiology 3
2.2 Neonatal Cardiovascular Pathophysiology 3
2.3 Recognition and Management of Neonatal Hemodynamic Compromise 3
2.4 Arterial Blood Pressure Waveform Analysis 4
2.4.1 Physiology of the Neonatal Arterial Blood Pressure Waveform 5
2.4.2 Advanced Arterial Blood Pressure Waveform Analysis 5
2.5 Measurement of the Arterial Blood Pressure Waveform 6
2.5.1 Dynamic Response of Catheter Manometer Systems 7
2.5.2 Effect of Dynamic Response on the Arterial Blood Pressure Waveform 8
3 Measurement of Dynamic Response Characteristics of Liquid-Filled Catheter Manometer Systems used in Neonatal Intensive Care: an In-Vitro Study 10
3.1 Introduction 10
3.2 Methods and Materials 10
3.2.1 Comparison of the Proximal Step Response and Flush Pulse Method with the Distal Step Response Method 11
3.2.2 The Influence of Different Catheter Manometer System Configurations and Air Bubbles on the Dynamic Response Characteristics 12
3.3 Results 13
3.4 Discussion 19
3.4.1 Comparison of the Proximal Step Response and Flush Pulse Method with the Distal Step Response Method 19
3.4.2 The Influence of Different Catheter Manometer System Configurations and Air Bubbles on the Dynamic Response Characteristics 19
3.4.3 Limitations and Recommendations 20
3.4.4 Clinical Implications 21
3.5 Conclusion 22
4 Accuracy of the Arterial Blood Pressure Waveform measured in Neonatal Intensive Care based on Dynamic Response Characteristics of Liquid-Filled Catheter Manometer Systems 23

4.1 Introduction 23
4.2 Methods and Materials 23
4.2.1 In-Vivo Measurement of Dynamic Response Characteristics 23
4.2.2 Evaluation of the Effect of the Total Monitoring Chain on the Neonatal Arterial Blood Pressure Waveform 24
4.2.3 Variability of DR characteristics over time 25
4.3 Results 25
4.3.1 In-Vivo Measurement of Dynamic Response Characteristics 25
4.3.2 Evaluation of the Effect of the Total Monitoring Chain on the Neonatal Arterial Blood Pressure Waveform 27
4.3.3 Variability of Dynamic Response Characteristics over Time 30
4.4 Discussion 32
4.4.1 Limitations and Recommendations 33
4.4.2 Clinical Implications 34
4.5 Conclusion 35
5 Reconstruction of the Arterial Blood Pressure Waveform measured in Neonatal Intensive Care based on Dynamic Response Characteristics of Liquid-Filled Catheter Manometer Systems 36
5.1 Introduction 36
5.2 Methods and Materials 37
5.3 Results 38
5.4 Discussion 40
5.5 Conclusion 42
6 Discussion 43
6.1 Strengths and Limitations 43
6.2 Future Perspectives 44
6.3 Conclusion 45
References 46
Appendix 51
A Derivation of the Equations for Natural Frequency and Damping Coefficient 51
B Derivation of the Step and Impulse Responses of the Monitoring System 52
C Calculation of Arterial Blood Pressure Waveform Parameters 53

1 Introduction

Hemodynamic compromise in neonates is associated with both short- and long-term adverse outcomes [1-5]. Causes of cardiovascular failure include inadequate transition from intra- to extrauterine life, persistent pulmonary hypertension of the newborn, hemodynamically significant patent ductus arteriosus, congenital heart defects, sepsis and systemic inflammatory diseases such as necrotizing enterocolitis [6]. Early and adequate treatment based on the underlying pathophysiology is important to prevent organ failure and death [7, 8]. Currently, assessment of neonatal hemodynamic status is mainly based on measurement of mean arterial blood pressure [9]. However, a clear definition of hypotension in the newborn population is lacking and the decision to provide treatment is highly variable among different centers [10]. Relying on mean blood pressure alone as indicator for hemodynamic compromise is limited due to the fact that mean blood pressure is a dependent variable, determined by the variables cardiac output (CO) and systemic vascular resistance (SVR) [6, 8]. Advanced hemodynamic monitoring may improve the ability to accurately and promptly identify the underlying pathophysiology of hemodynamic compromise and thereby guide the appropriate patient-specific treatment [8, 11-13].

Technologies developed for hemodynamic monitoring in adults are not always usable in neonates due to size constraints, the presence of shunts and potential adverse effects [12]. Neonatologist Performed Echocardiography (NPE) is currently the most used technique to estimate CO at the neonatal intensive care unit (NICU) [14]. However, such measurement requires specialized skill, cannot be performed continuously and may be inaccurate. There is growing interest in arterial pulse contour analysis techniques due to the benefit of using regular arterial lines [12]. At the NICU, blood pressure is routinely monitored invasively via an umbilical or peripheral arterial catheter. The continuously measured arterial blood pressure waveform (ABPW) is determined by the stroke volume (SV), vascular compliance, SVR and other physiological and physical factors [15]. Several algorithms are available to estimate SV from the ABPW, but no validation studies have been performed in neonates [12].

Importantly, advanced analysis of the ABPW requires a reliable and valid measurement method [16]. Although measurement of blood pressure using a liquid-filled catheter manometer system (CMS) is considered the gold standard in neonates, inadequate dynamic response (DR) of the CMS may distort the ABPW [17]. Possible causes of inadequate DR are the presence of small air bubbles in the catheter and too long or compliant tubing [18]. In adults, the DR characteristics can be determined with the fast flush test [19]. Based on these characteristics, it can be ascertained whether the ABPW is underdamped, overdamped or adequately measured. Unfortunately, the fast flush test is not applicable in neonates due to the risk of disturbing their fluid balance. Van Langen et al. [20] proposed an alternative method, the flush pulse test, but this method is not yet implemented into clinical practice at the NICU. Therefore, the DR characteristics of the CMS currently used at the NICU and their effect on the neonatal ABPW remain unknown. This effect may be even larger than the effect on the adult ABPW due to higher heart rates in neonates [17]. Identifying possible causes of inadequate DR response in neonatal intensive care may facilitate improvement of ABPW measurement. A measurement-specific reconstruction method for distorted ABPW was previously proposed, but requires further validation before it can be implemented in clinical practice [21, 22].

1.1 Aim and Objectives

The primary aim of this study is to evaluate the accuracy of the ABPW measured in neonatal intensive care based on DR characteristics of liquid-filled CMS. To improve the accuracy of the measured ABPW, the secondary aim is to provide the initial validation of a reconstruction method for ABPW in case of inadequate DR.

In order to achieve these aims, the following objectives are formulated:

1. Validate a method for assessing the DR characteristics of CMS currently used at the NICU,
2. Measure the in-vivo DR characteristics of CMS at the NICU using the validated method,
3. Simulate the effect of the total monitoring chain on the neonatal ABPW,
4. Explore the variability of DR characteristics of CMS at the NICU,
5. Identify possible causes of inadequate DR of CMS at the NICU,
6. Initially validate a measurement-specific reconstruction method for ABPW in case of inadequate DR.

1.2 Thesis Outline

In chapter 1, a general introduction to this thesis is given. More elaborate background information is provided in chapter 2. Chapter 3 describes an in-vitro validation study of two methods for the in-vivo assessment of DR characteristics. Furthermore, possible causes of inadequate DR are identified. In chapter 4, the accuracy of the measured neonatal ABPW is evaluated based on the in-vivo measured DR characteristics and computer simulations of the total monitoring chain. Besides, the variability of DR characteristics of CMS is explored. In chapter 5, a measurement-specific reconstruction method for distorted ABPW is proposed and initially validated. Finally, chapter 6 provides a general discussion and conclusion of all the results obtained in this thesis.

2 Background

2.1 Developmental Cardiovascular Physiology

During feto-neonatal transition, substantial cardiovascular changes occur [14, 23]. Since the fetal lungs are not inflated with air, gas exchange occurs via the placenta. In order to deliver oxygenated blood from the umbilical veins to the systemic circulation, blood flows through the foramen ovale (FO) between the right and left atria and through the ductus arteriosus between the pulmonary artery and aorta. Due to the presence of these shunts and a high pulmonary vascular resistance (PVR), fetal pulmonary blood flow (PBF) is low. In the first few minutes of life, inflation of the lungs and umbilical cord clamping cause a decrease in PVR and increase in systemic vascular resistance (SVR), respectively. The subsequent increase in PBF and left atrial pressure results in the functional closure of the FO. In healthy term infants, functional closure of the ductus arteriosus occurs by smooth muscle constriction within the first hours after birth, while anatomical closure occurs over the next several days [24].
The primary goal of the cardiovascular system is delivery of oxygen and nutrients to cells to meet their metabolic needs and removal of carbon dioxide and metabolic waste from the tissue [14]. Oxygen delivery is determined by cardiac output (CO) and the arterial oxygen content. Importantly, oxygen can only be delivered effectively if an adequate perfusion pressure is maintained [7]. According to Ohm's law, perfusion pressure is determined by the product of CO and SVR. CO is the product of heart rate and stroke volume (SV) [14]. The latter is determined by preload, contractility and afterload. Preload can be described as the extent of initial stretching of cardiac muscle fibers prior to myocardial contraction and is determined by venous return and ventricular compliance. Contractility refers to the intrinsic contractile strength of the myocardium, independent of preload. Afterload is defined as the force that the heart must overcome prior to ejection of the SV and is determined by ventricular dimensions, SVR and vascular compliance. Lastly, SVR is determined by the resistance of small vessels, mainly arterioles [7]. Changes in the vascular tone of arterioles through local, paracrine and neurohormonal factors regulate organ blood flow. From the described cardiovascular physiology it is clear that blood pressure is the result of a complex interplay between cardiac and vascular factors.

2.2 Neonatal Cardiovascular Pathophysiology

When oxygen delivery to the tissues does not meet its demand, shock occurs [7]. This can be caused by inadequate cardiac output, dysregulation of vascular tone, or both [6, 8]. A reduced cardiac output is due to rhythm, preload, contractility or afterload issues. The leading cause of hemodynamic compromise in the neonatal population is low SVR due to peripheral vasodilatation, which occurs in septic shock or systemic inflammatory diseases such as necrotizing enterocolitis [6]. Furthermore, shock might be caused by inadequate feto-neonatal transition [25]. While in most term infants this transition occurs smoothly, premature infants have limited capacity to adjust to the hemodynamic challenges in the immediate postnatal period [26]. Immediate cord clamping leads to a sudden increase in afterload combined with a decrease in preload. The limited ability of the immature myocardium to subsequently increase contractility may lead to inadequate cardiac output. In addition, perinatal asphyxia may cause a decrease in myocardial contractility [27]. Besides, a patent ductus arteriosus (PDA), which is common in preterm infants, causes a left-to-right shunt and thereby a decreased systemic blood flow (SBF) in case of a low PVR and high SVR [14]. Ligation of a PDA results in an increased afterload and can therefore cause further hemodynamic instability.

2.3 Recognition and Management of Neonatal Hemodynamic Compromise

In the compensated phase of shock, perfusion of vital organs is maintained through local vasodilatation, whereas nonvital organ perfusion has decreased through selective vasoconstriction

[7]. This phase is characterized by preserved normal blood pressure, increased heart rate, cold extremities, delayed capillary refill time and decreased urine output. Although these clinical signs aid in the early detection of shock in pediatric and adult patients, their value is limited in the neonatal population. Assessment of hemodynamic status at the neonatal intensive care unit (NICU) relies mainly on measurement of mean blood pressure [9]. Therefore, shock is usually only recognized in the uncompensated phase, when compensatory mechanisms fail and hypotension occurs [7]. Treatment is aimed at restoring adequate organ perfusion, especially cerebral blood flow, based on the observed association between hypotension and neuromorbidity [9]. However, inappropriate choice and titration of antihypotensive therapy may cause reperfusion injury, especially in preterm infants with reduced cerebral autoregulation [6, 8, 11]. Unfortunately, due to challenges in conducting randomized controlled trials, there is a paucity of evidence regarding the appropriate therapy of neonatal shock [6, 11, 13]. Therefore, treatment strategies targeted to the major hemodynamic parameter causing cardiovascular compromise should be considered [8]. While inotropes primarily increase myocardial contractility and thereby CO, vasoactive drugs increase or decrease the vascular tone and thereby influence the SVR. Most of the medications used at the NICU have combined inotropic and vasoactive effects, albeit to a varying degree [11]. Thus, obtaining information on the CO and SVR through advanced hemodynamic monitoring is important to guide individualized treatment [6, 11, 13]. This may be achieved through advanced analysis of the arterial blood pressure waveform (ABPW).

2.4 Arterial Blood Pressure Waveform Analysis

At the NICU, blood pressure can be measured non-invasively with oscillometric techniques or invasively via an in-dwelling intra-arterial catheter [28]. Intra-arterial catheterization is indicated for continuous blood pressure monitoring in unstable critically ill neonates, frequent arterial blood sampling or exchange transfusions. The catheter is placed in the umbilical or a peripheral artery, usually the radial, ulnar or posterior tibial artery. In infants, the ABPW is similar in central and peripheral arteries [29, 30]. Figure 2.1 shows a characteristic neonatal ABPW measured with a high-fidelity system by Gevers et al. [31].

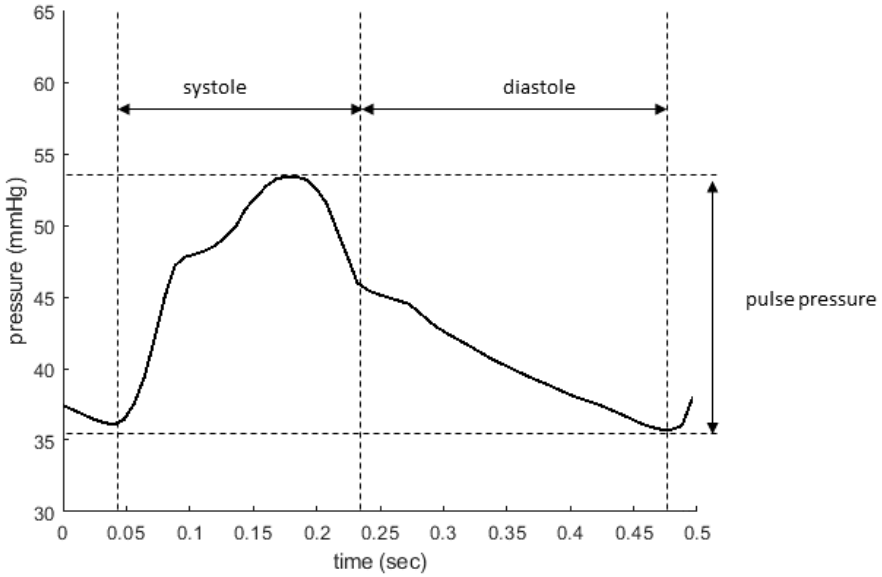

Figure 2.1: Characteristic neonatal arterial blood pressure waveform measured with a high-fidelity system. The dicrotic notch indicates the end of systole and beginning of diastole. The pulse pressure is the difference between the systolic and diastolic pressures.

In current clinical practice, mainly the mean pressure and, to a lesser extent, the pulse pressure (PP) are derived from the ABPW measured in neonates. Advanced analysis of the ABPW may reveal more clinically relevant information about the cardiovascular status [32, 33].

2.4.1 Physiology of the Neonatal Arterial Blood Pressure Waveform

Each component of the ABPW is based on dynamic interactions between the heart and vasculature, called ventricular-vascular coupling [33]. Ejection of blood from the left ventricle into the aorta during systole causes a steep rise or upstroke of arterial pressure to the peak systolic pressure, which is mainly determined by the left ventricular SV and vascular compliance. This is followed by a decrease in pressure at the end of systole and during diastole. The diastolic pressure primarily depends on the ability of the proximal arteries to recoil and the SVR. The incisura, or dicrotic notch, represents the closure of the aortic valve and thereby marks the end of systole. Since neonates have highly compliant arteries, this population generally has lower systolic and higher diastolic blood pressures, resulting in lower PP. Furthermore, the dicrotic notch is less prominent than in adults. Sometimes an anacrotic notch can be discerned, either before (A-type) or after (C-type) the systolic peak [34]. These are the result of wave reflections, which are mainly determined by arterial compliance and geometry [35]. In neonates mostly A-type augmentation is visible [29], which can be explained by their relatively long ventricular ejection period and early return of reflected waves from peripheral to central vessels due to short body length [30, 36].

2.4.2 Advanced Arterial Blood Pressure Waveform Analysis

In pulse contour analysis, usually the PP or area under the systolic portion of the waveform are used to estimate SV and thereby CO [33]. However, the relationship between these parameters is influenced by the vascular compliance and resistance. Three different types of devices have been developed [15]. The first one requires frequent external calibration with an independent method for CO measurement, such as transpulmonary thermodilution, which is not feasible in neonates. The second one is internally calibrated, based on biometric, demographic and hemodynamic data, but is less reliable compared to externally calibrated devices [32]. The only device that does not require frequent calibration is based on the pressure recording analytical method (PRAM) algorithm, in which so-called ‘points of instability’ in the ABPW are analyzed to estimate vascular compliance and resistance. However, no validation studies of the PRAM in neonates have been performed and validation studies in critically ill children provided conflicting results [37, 38].

Besides the PP and systolic area under the curve (AUC), the slope of the systolic upstroke and dicrotic notch have been parameters of interest in several studies. The slope of the systolic upstroke reflects the change in pressure over time, or dP/dt, during ventricular ejection [32]. The steeper this slope, the stronger the contractile forces of the heart appear. Although left ventricular (LV) maximal dP/dt is generally accepted as a marker of LV contractility, the relationship between peripheral maximal dP/dt and LV contractility may be affected by other hemodynamic factors [39]. Nevertheless, Monge Garcia et al. showed that radial and particularly femoral maximal dP/dt is sensitive to changes in LV contractility during different pre- and afterloading conditions in pigs [40]. Therefore, analysis of the peripheral ABPW in neonates, which is more similar to the central ABPW, may be more useful for evaluation of LV contractility than the peripheral ABPW measured in adults. Furthermore, the aortic ABPW can be measured in neonates using an umbilical catheter.

The dicrotic notch indicates closure of the aortic valve, which occurs when aortic blood pressure exceeds LV blood pressure. In case of reduced SVR, this can only be achieved later in the cardiac cycle, leading to a lower and delayed dicrotic notch [33]. This is supported by clinical data, as an increased dicrotic notch pressure is seen after administering vasoconstrictive medication [41]. Also in premature

infants with a high transductal left-to-right shunting volume, a lower and delayed dicrotic notch has been observed [42].

2.5 Measurement of the Arterial Blood Pressure Waveform

Advanced analysis of the ABPW requires a reliable and valid measurement method. Invasive blood pressure sensor systems can be divided into two general categories based on the location of the sensor element [43]. In liquid-filled catheter manometer systems (CMS), blood pressure is transmitted to an external sensor element via a liquid-filled catheter. In the other category, known as manometer tipped catheters (MTC), the liquid coupling is eliminated by incorporating the sensor into the tip of the catheter. An MTC is more expensive and may break after only a few uses, further increasing its cost per use. Therefore, a liquid-filled CMS is currently used for invasive blood pressure measurement at the NICU. The measurement system is schematically shown in Figure 2. The liquid-filled CMS consists of a cannula or catheter placed in the artery connected to a disposable transducer and blood sampling set. The 150 cm long tubing incorporating a blood sampling port facilitates the pressure transducer to be placed outside the incubator or crib. An infusion pump provides a continuous flow of saline-heparin solution through the transducer and tubing to the patient to prevent blood from clotting at the tip. The flush valve can be opened with a lever to increase the flow. An increase in pressure at the cannula tip leads to displacement of a diaphragm in the silicon chip, which is sensed by a strain gage. The subsequent electrical signal is amplified and filtered with a low pass filter by the patient monitor [44]. The electrical connections are protected from the saline by a compliant silicone elastomer gel, which also provides electrical isolation [45].

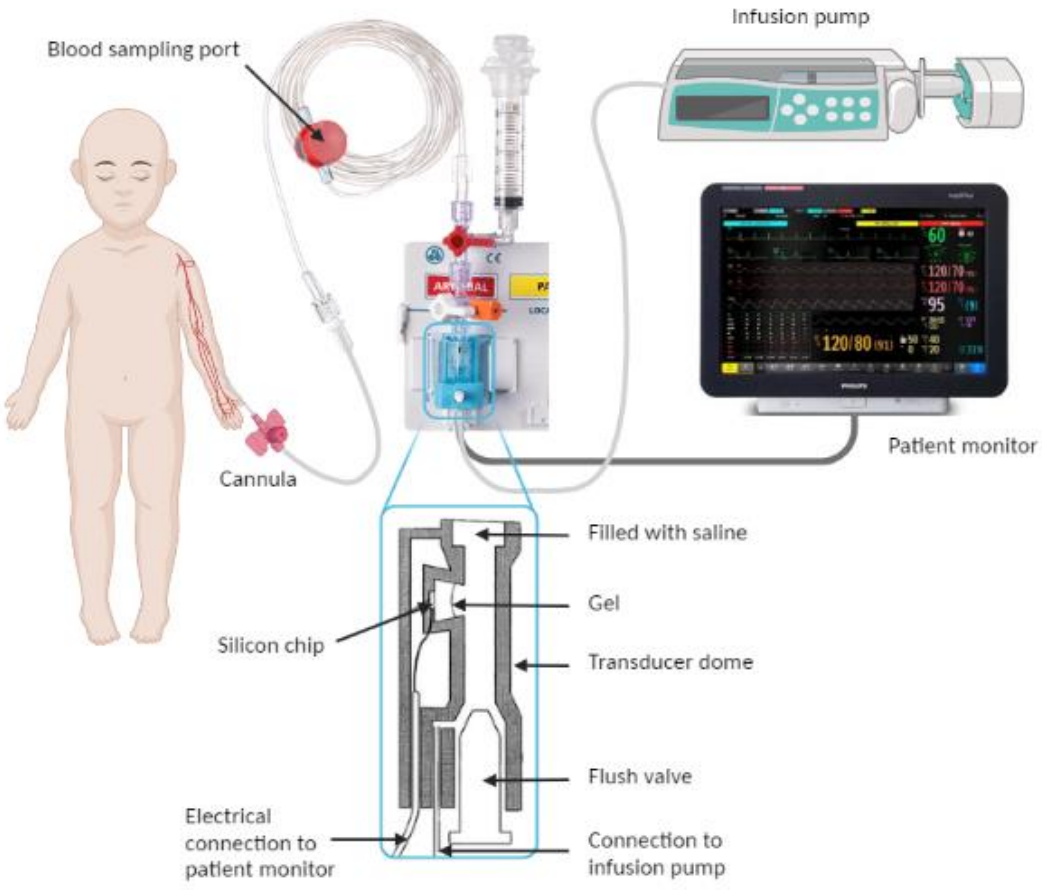

Figure 2.2: Schematic, not-to-scale, overview of invasive blood pressure measurement via liquid-filled catheter manometer systems at the neonatal intensive care unit. Modified from [43].

2.5.1 Dynamic Response of Catheter Manometer Systems

A liquid-filled CMS can be modelled by the simplified analogous electrical circuit shown in Figure 2. [43]. It is assumed that the compliance of the sensor diaphragm is much larger than that of the liquid-filled catheter and sensor cavity for a bubble-free, noncompliant catheter. Furthermore, the resistance and inertance of the catheter are larger compared to those of the sensor, due to the longer length and smaller diameter.

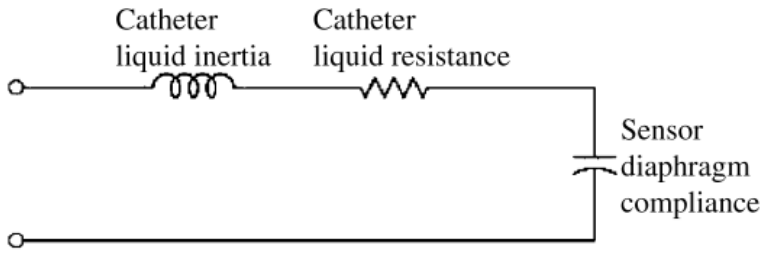

Figure 2.3: Simplified analogous electrical circuit of a liquid-filled catheter manometer system [43].

The catheter liquid inertia (L_c) can be described by

$$L_c = \frac{\rho L}{\pi r^2}, \tag{Eq. 2.1}$$

where ρ is the fluid density, and L and r are the length and radius of the catheter, respectively. According to Poiseuille's equation, the catheter liquid resistance (R_c) can be calculated by

$$R_c = \frac{8\eta L}{\pi r^4}, \tag{Eq. 2.2}$$

with η the fluid viscosity. Lastly, the sensor diaphragm compliance (C_d) is given by

$$C_d = \frac{\Delta V}{\Delta P} = \frac{1}{K}, \tag{Eq. 2.3}$$

where ΔV is the change in volume, ΔP is the change in pressure, and K is the elastance of the sensor diaphragm.

Using this analogous electrical circuit, a CMS can be modelled as a second-order dynamic system, characterized by a natural frequency (f_n) and damping coefficient (ζ) according to the following equation:

$$\frac{d^2O(t)}{dt^2} + 2\omega_n\zeta\frac{dO(t)}{dt} + \omega_n^2 O(t) = \omega_n^2 I(t), \tag{Eq. 2.4}$$

with $I(t)$ the input signal, analogous to the applied pressure, $O(t)$ the output signal, analogous the pressure sensed at the diaphragm and $\omega_n = 2\pi f_n$ the natural angular frequency. Using Kirchhoff's voltage law and Equations 2.1, 2.2 and 2.3, it can be shown that the natural frequency and damping coefficient are given by (see Appendix A):

$$f_n = \frac{r}{2}\sqrt{\frac{K}{\pi\rho L}}, \tag{Eq. 2.5}$$

and

$$\zeta = \frac{4\eta}{r^3}\sqrt{\frac{L}{\pi\rho K}}. \tag{Eq. 2.6}$$

2.5.2 Effect of Dynamic Response on the Arterial Blood Pressure Waveform

Although blood pressure measurement with a liquid-filled CMS is currently considered the gold standard in neonates, inadequate dynamic response (DR) of the CMS may distort the ABPW [17]. Every ABPW can be divided into its fundamental frequency and a weighted sum of higher harmonics (see Figure 2.4). For accurate measurement of the ABPW, it is generally accepted that up to the tenth harmonic should be preserved, which can be 30 Hz for neonates [46]. Depending on the natural frequency and damping coefficient of the CMS, frequency components of the ABPW may be enhanced or attenuated. In adults, most CMS cause underdamping of the ABPW (see Figure 2.5) [47]. However, the CMS used at the NICU may have different DR characteristics. Furthermore, the effect of certain DR characteristics on neonatal ABPW may be different from the effect on adult ABPW due to differences in heart rate and slope of the systolic upstroke [48]. Therefore, it is important to assess the in-vivo DR characteristics of CMS currently used at the NICU and their effect on the neonatal ABPW.

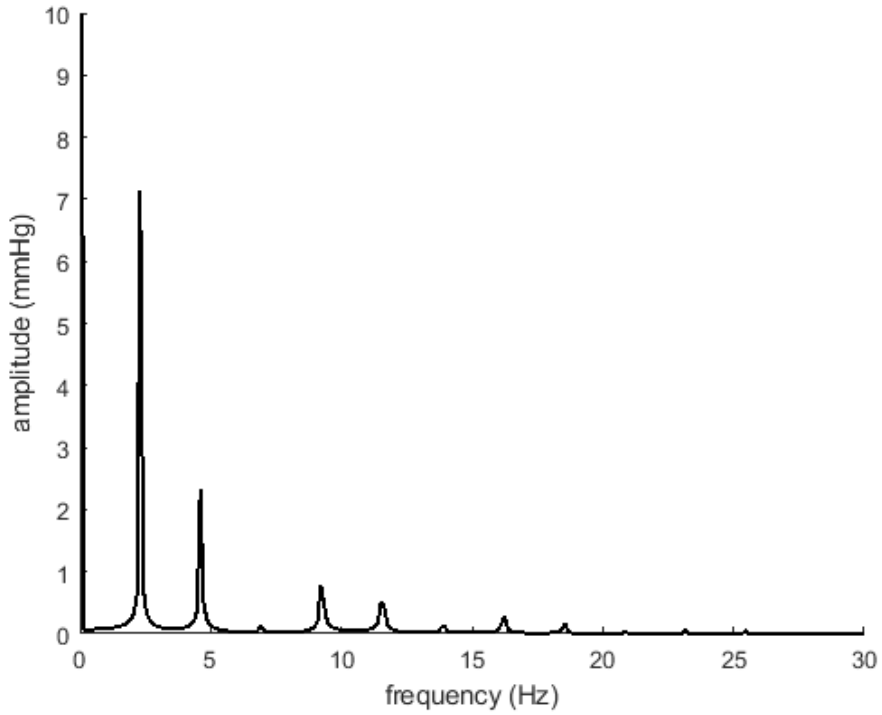

Figure 2.4: Amplitude spectrum of the characteristic neonatal arterial blood pressure waveform shown in Figure 2.1. The amplitude at zero frequency is out of range, because the graph was magnified to visualize the amplitudes of the higher harmonics.

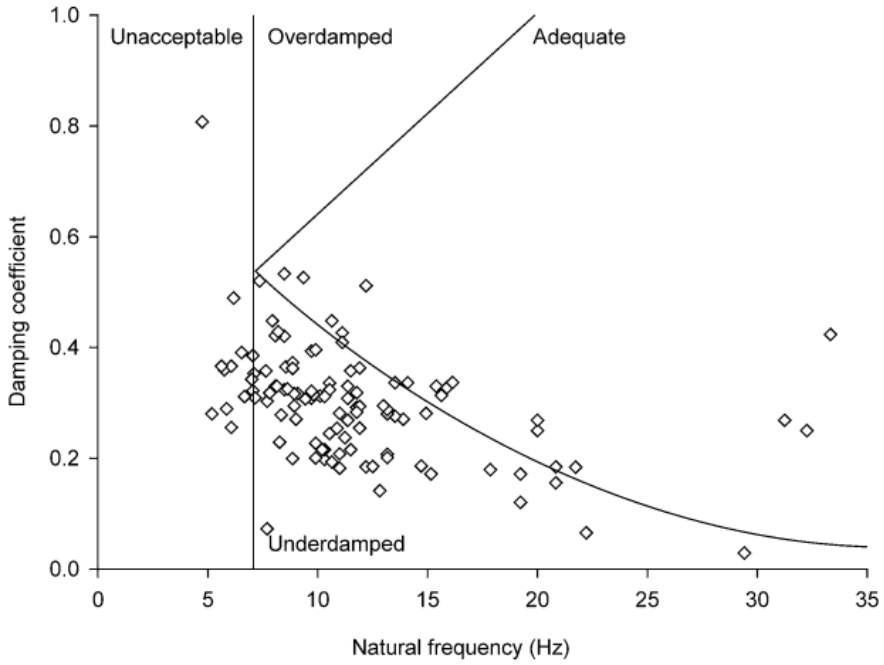

Figure 2.5: Dynamic response characteristics of liquid-filled catheter manometer systems measured in adults [47].

3 Measurement of Dynamic Response Characteristics of Liquid-Filled Catheter Manometer Systems used in Neonatal Intensive Care: an In-Vitro Study

3.1 Introduction

Advanced analysis of the arterial blood pressure waveform (ABPW) in neonates requires an accurate measurement method. Measuring blood pressure with a liquid-filled catheter manometer system (CMS) is currently considered the gold standard in neonates [18]. However, the measured ABPW may be distorted by an inadequate dynamic response (DR) of the CMS, determined by its natural frequency and damping coefficient [17]. Possible causes of an inadequate DR are the presence of small air bubbles or blood in the CMS and too long or too compliant tubing [18, 19]. In adults, the fast flush method can be used to assess the DR characteristics of the whole CMS in situ [49, 50]. Opening and closing of the flush device exposes the system to a sudden pressure change, thereby generating a step response. From the measured step response, the natural frequency and damping coefficient can be determined, based on the assumption that the whole measurement system can be modelled as an underdamped second-order dynamic system. Unfortunately, the fast flush method is not applicable in neonates due to the risk of disturbing their fluid balance. Therefore, Van Langen et al. proposed the flush pulse method, in which opening and releasing of the flush valve elicits an impulse response, without affecting the infant's circulation [20]. Validation in laboratory settings showed good agreement between the results obtained with the flush pulse method and a generally accepted reference method, in which a step response is generated at the distal end of the CMS. Nevertheless, it is important to validate this method for the currently used CMS, since these are probably different from those used by Van Langen et al. [20].

Although the flush pulse method requires an easy intervention, it is not routinely performed at the neonatal intensive care unit (NICU). Alternatively, it was observed that the sudden release of pressure in the CMS after routine blood sampling generates a step response, which may facilitate the measurement of DR characteristics retrospectively. However, due to the generation of a proximal instead of distal step response, this method may not reflect the DR characteristics of the whole CMS [51]. Hence, this method should also be validated against the distal step response method. Furthermore, it should be recognized that the patient monitor that is connected to the transducer, commonly applies a low pass filter to the measured ABPW [51]. Thus, the whole monitoring chain should be regarded as a third or higher order system.

The primary aim of this in-vitro study is to compare the flush pulse method of Van Langen et al. [20] and the proposed proximal step response method with the distal step response method as reference for measuring the DR characteristics of CMS currently used at the NICU. Both the flush pulse method and proximal step response method will be performed using two different cut-off frequencies of the monitor low pass filter, to investigate whether this will influence the accuracy of either method. The secondary aim is to investigate the influence of different CMS configurations and the presence of small air bubbles on the DR characteristics.

3.2 Methods and Materials

The experimental setup that was used is shown in Figure 3.1. The disposable pressure transducer and blood sampling set (Safedraw^{TM}-P, Merit Medical^{TM}, Galway, Ireland), currently used at the NICU at the Radboudumc Amalia Children's Hospital for blood pressure measurement, incorporates a closed blood sampling port at the distal end of the 150 cm long extension tubing. This system was carefully filled with a 0.9% saline solution. Remaining visible air bubbles were removed by gently tapping the

transducer dome and tubing. The flow rate, controlled by an infusion pump, was subsequently set to 1 mL/h. The pressure transducer was mounted on an intravenous pole mounting plate and electrically connected to a patient monitor (IntelliVue MP90, Philips Medical Systems, Cambridge, Massachusetts, United States). The transducer was zeroed according to the manufacturer's instructions before the measurements were started. The measured signals were extracted from the monitor using the open source VitalSignsCapture software, with a sampling frequency of 250 Hz, and subsequently analyzed using Matlab (MATLAB R2022a, The MathWorks, Inc., Natick, Massachusetts, United States).

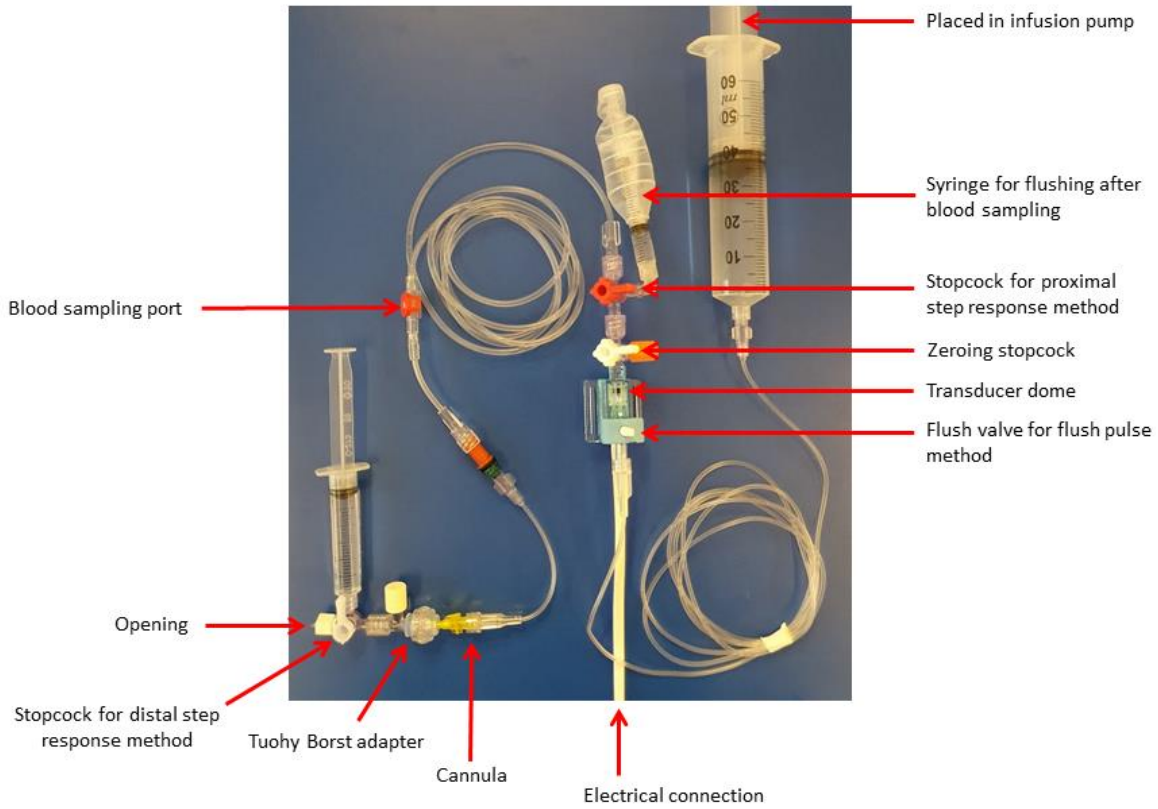

Figure 3.1: Experimental setup to determine the dynamic response characteristics of catheter manometer systems in-vitro with the proximal step response method, the flush pulse method and the distal step response method. The lines are rolled up and the infusion pump and mounting plate are removed for visualization purposes.

3.2.1 Comparison of the Proximal Step Response and Flush Pulse Method with the Distal Step Response Method

To generate a distal step response, the tip of the cannula or catheter was placed inside a Tuohy Borst adapter (FLO40™, Merit Medical™, Galway, Ireland) filled with saline and the valve membrane was tightened to prevent pressure loss. A three-way stopcock was connected to the other end of the Tuohy Borst adapter. By closing of the opening to the atmosphere and pushing the plunger of the syringe, the pressure inside the Tuohy Borst adapter was increased to 200 mmHg. Turning the stopcock 90 degrees suddenly released the pressure to atmospheric pressure, thereby eliciting a distal step response which was measured by the transducer. To generate a proximal step response such as observed during blood sampling, the red three-way stopcock was closed to the transducer and the flow rate of the infusion pump was briefly increased, so that the pressure measured by the transducer increased to 200 mmHg. Then, the stopcock was closed to the sampling syringe, which again led to a sudden drop in pressure. For the flush pulse method, the three-way stopcocks were positioned as shown in Figure 3.1. The flush valve was briefly opened and then released, which elicited an impulse response in the system.

The three different responses were recorded by the patient monitor. For the distal step response, the cut-off frequency of the monitor low pass filter was set as high as possible to 40 Hz, to limit the distortion caused by the filter. The proximal step response and flush pulse response were recorded with both a cut-off frequency of 12 Hz and 40 Hz. The low pass filter was assumed to be a second-order Butterworth filter. Therefore, the total monitoring chain was considered as the sum of two second-order underdamped systems and the step or impulse response can be given by (see Appendix B for the derivation):

$$P(t) = A \cdot e^{-2\pi f_n \zeta t} \cdot \sin\left(2\pi f_n \cdot \sqrt{1-\zeta^2} \cdot t + B\right) + C \cdot e^{-2\pi f_c \frac{\sqrt{2}}{2} t} \cdot \sin\left(2\pi f_c \cdot \frac{1}{\sqrt{2}} \cdot t + D\right) + E, \quad \text{(Eq. 3.1)}$$

with $P(t)$ the measured response in mmHg, t the time in seconds, f_c the cut-off frequency of the Butterworth low pass monitor filter in Hz and A (in mmHg), B, C (in mmHg), D and E (in mmHg) being constants. The natural frequency f_n in Hz and damping coefficient ζ can be derived from the measured response by fitting Equation 3.1. When measuring the proximal step response or flush pulse in-vivo, the response will be superimposed on the ABPW. Analyzing the first derivative of the response will reduce the influence of disturbances related to the underlying ABPW as proposed by van Langen et al [20]. Taking the first derivative of Equation 3.1 gives a similar equation, with $P(t)$ replaced by $dP/dt(t)$ in mmHg/s and A, C and E in mmHg/s instead of mmHg. Therefore, Equation 3.1 can also be fitted to the first derivative of the measured responses, provided that high-frequency noise is removed by the monitor low pass filter so that amplification of noise by taking the first derivative is limited. For validation purposes, the DR characteristics were calculated from the first derivative of the proximal step responses and flush pulses, while for the distal step response method the pressure signal itself was analyzed.

3.2.2 The Influence of Different Catheter Manometer System Configurations and Air Bubbles on the Dynamic Response Characteristics

The different response methods were evaluated using four different cannula or catheter types: a 24-gauge (24G) cannula (Vigmed, Helsingborg, Sweden), 26G cannula (Vigmed, Helsingborg, Sweden), 3.5-french (3.5F) 40 cm long catheter (Vygon, Ecouen, France) and 2.5F 30 cm long catheter (Vygon, Ecouen, France). The 24G and 26G cannulas were connected to the transducer set via an extra extension tube with a length of 13 cm, simulating the real clinical setting. Next to this, the different responses were measured after adding another 200 cm long extension line to the 24G cannula, which is used during surgery to keep the blood sampling port away from the sterile field.

For each CMS configuration and response method, the natural frequency and damping coefficient were determined by taking the average of three consecutive measurements. Furthermore, these measurements were repeated for three different transducer and blood sampling sets. Finally, the influence of a small visible air bubble on the measured natural frequency and damping coefficient was evaluated in one CMS with a 24G cannula. The DR characteristics were determined in four different situations: prior to injection of the air bubble, after injection when the air bubble was visible inside the transducer dome (see Figure 3.2), when the air bubble was moved to the blood sampling port, and when the air bubble was removed from the CMS.

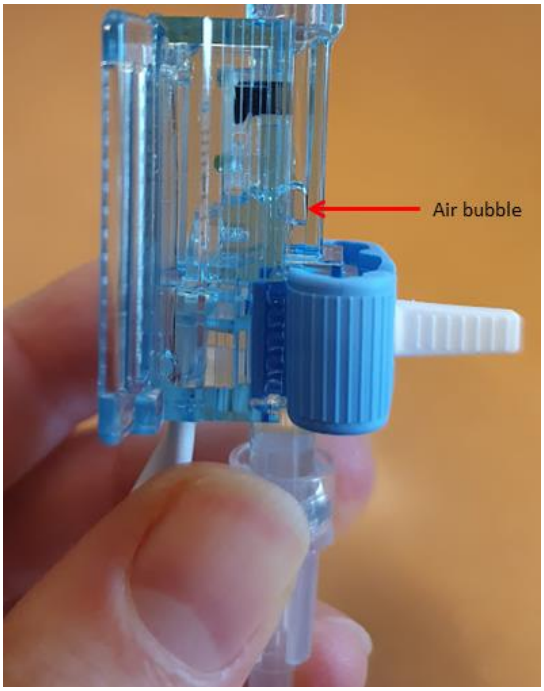

Figure 3.2: Air bubble visible in the transducer dome.

3.3 Results

Examples of the measured responses and fitted curves using the different methods and a 40 Hz low pass monitor filter are shown in Figures 3.3, 3.4 and 3.5.

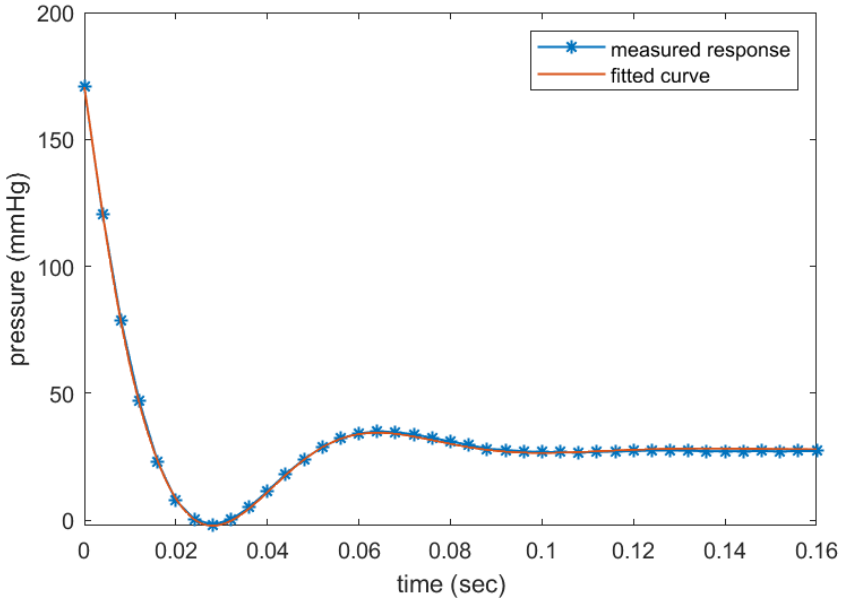

Figure 3.3: Example of the measured response and fitted curve using the distal step response method. Individual measurement points are indicated with asterisks.

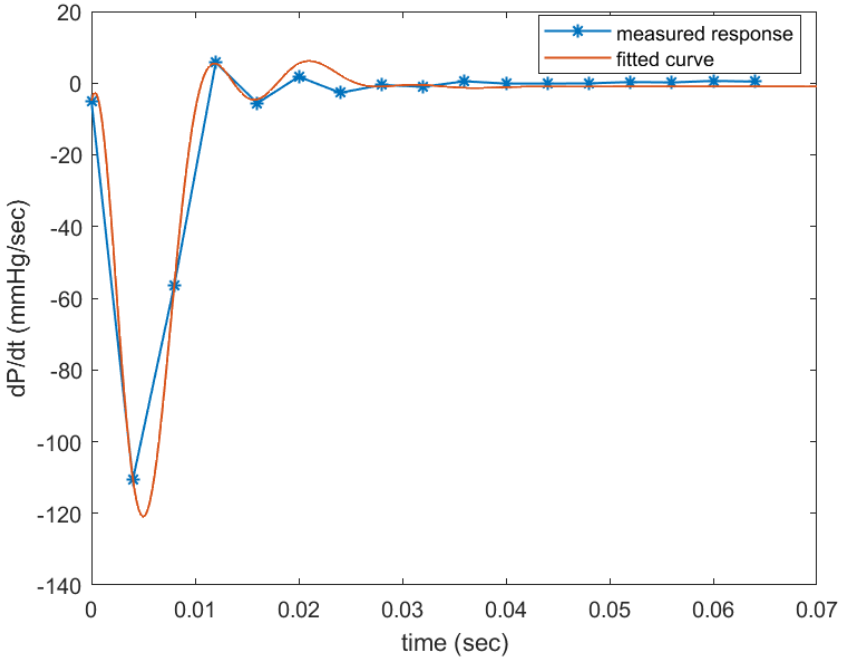

Figure 3.4: Example of the first derivative of the measured response and fitted curve using the proximal step response method with a monitor low pass filter of 40 Hz. Individual measurement points are indicated with asterisks.

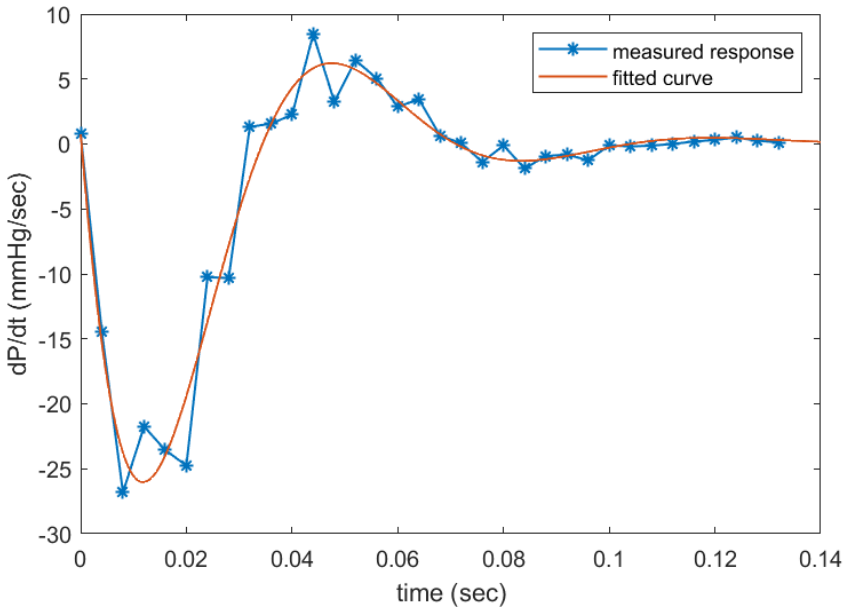

Figure 3.5: Example of the first derivative of the measured response and fitted curve using the flush pulse method with a monitor low pass filter of 40 Hz. Individual measurement points are indicated with asterisks.

The measured natural frequencies and damping coefficients for the different types of catheters and using the different response methods are shown in Tables 3.1 and 3.2 respectively. With the 2.5F catheter and when using the proximal step response method with a 12 Hz monitor low pass filter, non-oscillating exponentially decaying responses were seen, implying a damping coefficient of ≥ 1.0. Table 3.1 shows that the measured natural frequencies using the proximal step response method with a 40 Hz low pass filter were consistently higher compared to the measurements using the distal step response method. The average difference between these two methods was 99.5 Hz. The average differences between the measured natural frequencies using the flush pulse method and the distal

step response method were much smaller, namely 2.6 Hz and 3.9 Hz when using respectively the 40 Hz and 12 Hz monitor low pass filter. For the measured damping coefficients, the average differences between the distal step response method and the flush pulse method were 0.07 respectively 0.08 for the 40 Hz and 12 Hz monitor low pass filters. The average DR characteristics measured using these response methods are visualized in Figure 3.6. This figure shows that the higher the natural frequency, the larger the difference in measured DR characteristics between the different transducer and blood sampling sets as well as the different response methods. The natural frequencies measured using the flush pulse method were lower compared to the values measured using the distal step response, except for the natural frequency measured with the 12 Hz low pass filter after adding the extension line. Adding the extension line more than halved the natural frequency, while the damping coefficient almost doubled. Furthermore, Figure 3.6 shows that the natural frequency measured with the 3.5F catheter was lower compared to those measured with the 24G and 26G cannulas.

Table 3.1: In-vitro measured natural frequencies for different types of catheters and using different response methods. The measurements were repeated for three different transducer and blood sampling sets. Mean (minimal - maximal) values of three consecutive measurements in each set are shown. Furthermore, the mean values of the three different sets were averaged again and shown. N/O = no oscillation.

Cannula or catheter type	Trans-ducer and blood sampling set	Natural frequency (Hz)				
		Distal step response method with 40 Hz low pass filter	Proximal step response method		Flush pulse method	
			40 Hz low pass filter	12 Hz low pass filter	40 Hz low pass filter	12 Hz low pass filter
24G cannula	1	36.7 (35.1 – 37.7)	125.2 (111.1 – 138.3)	N/O	37.1 (35.2 – 38.3)	34.0 (37.1 – 38.4)
	2	37.0 (35.1 – 38.8)	125.6 (121.6 – 129.3)	N/O	38.4 (37.0 – 39.4)	35.7 (35.6 – 35.7)
	3	44.3 (42.8 – 45.8)	131.4 (128.1 – 137.0)	N/O	38.0 (37.1 – 38.9)	34.4 (33.7 – 35.1)
	Average	39.4	127.4	N/O	37.8	34.7
26G cannula	1	41.3 (39.3 – 43.1)	127.7 (125.8 – 130.6)	N/O	39.7 (36.5 – 41.6)	39.1 (38.9 – 39.4)
	2	40.3 (34.4 – 46.2)	123.1 (119.8 – 124.7)	N/O	37.7 (37.2 – 38.0)	33.7 (33.6 – 33.8)
	3	42.6 (40.3 – 46.9)	130.6 (127.9 – 134.1)	N/O	35.4 (34.8 – 35.8)	33.7 (33.0 – 34.3)
	Average	41.4	127.1	N/O	37.7	35.5
3.5F catheter	1	29.0 (28.0 – 29.9)	133.0 (131.7 – 134.8)	N/O	25.7 (25.3 – 26.0)	26.3 (26.1 – 26.6)
	2	28.6 (28.3 – 29.0)	132.4 (129.9 – 136.0)	N/O	25.1 (25.0 – 25.1)	25.6 (25.4 – 25.9)
	3	30.4 (30.0 – 30.6)	135.5 (131.8 – 141.8)	N/O	26.9 (26.5 – 27.4)	26.8 (26.1 – 27.3)
	Average	29.3	133.6	N/O	25.9	26.2
2.5F catheter	1	N/O	129.5 (129.1 – 130.1)	N/O	N/O	N/O
	2	N/O	129.3 (127.5 – 130.4)	N/O	N/O	N/O
	3	N/O	139.0 (132.9 – 142.7)	N/O	N/O	N/O
	Average	N/O	132.6	N/O	N/O	N/O
24G cannula + extension line	1	15.3 (15.3 – 15.3)	133.3 (130.6 – 138.3)	N/O	14.7 (13.9 – 15.1)	17.0 (16.2 – 18.5)
	2	13.6 (13.3 – 14.0)	134.4 (129.9 – 141.4)	N/O	14.2 (13.3 – 15.9)	16.5 (15.3 – 17.1)
	3	15.3 (15.1 – 15.6)	136.0 (131.5 – 138.6)	N/O	15.1 (14.9 – 15.3)	17.1 (16.1 – 17.8)
	Average	14.7	134.6	N/O	14.7	16.9

Table 3.2: In-vitro measured damping coefficients for different types of catheters and using different response methods. The measurements were repeated for three different transducer and blood sampling sets. Mean (minimal - maximal) values of three consecutive measurements in each set are shown. Furthermore, the mean values of the three different sets were averaged again and shown.

Cannula or catheter type	Trans-ducer and blood sampling set	Damping coefficient				
		Distal step response method with 40 Hz low pass filter	Proximal step response method		Flush pulse method	
			40 Hz low pass filter	12 Hz low pass filter	40 Hz low pass filter	12 Hz low pass filter
24G cannula	**1**	0.24 (0.22 – 0.26)	0.32 (0.21 – 0.49)	≥ 1.0	0.29 (0.28 – 0.32)	0.28 (0.23 – 0.34)
	2	0.27 (0.24 – 0.29)	0.33 (0.25 – 0.38)	≥ 1.0	0.23 (0.21 – 0.24)	0.22 (0.22 – 0.23)
	3	0.25 (0.21 – 0.28)	0.32 (0.28 – 0.35)	≥ 1.0	0.38 (0.37 – 0.39)	0.27 (0.25 – 0.28)
	Average	0.25	0.32	≥ 1.0	0.30	0.26
26G cannula	**1**	0.40 (0.28 – 0.53)	0.26 (0.24 – 0.29)	≥ 1.0	0.39 (0.27 – 0.61)	0.16 (0.11 – 0.19)
	2	0.32 (0.29 – 0.34)	0.23 (0.20 – 0.26)	≥ 1.0	0.46 (0.43 – 0.51)	0.28 (0.26 – 0.32)
	3	0.20 (0.17 – 0.26)	0.33 (0.27 – 0.38)	≥ 1.0	0.46 (0.37 – 0.56)	0.28 (0.28 – 0.29)
	Average	0.31	0.27	≥ 1.0	0.44	0.24
3.5F catheter	**1**	0.31 (0.29 – 0.33)	0.38 (0.34 – 0.42)	≥ 1.0	0.28 (0.23 – 0.31)	0.22 (0.21 – 0.22)
	2	0.39 (0.37 – 0.41)	0.44 (0.33 – 0.59)	≥ 1.0	0.30 (0.28 – 0.32)	0.27 (0.24 – 0.29)
	3	0.30 (0.29 – 0.31)	0.42 (0.41 – 0.43)	≥ 1.0	0.29 (0.28 – 0.30)	0.23 (0.22 – 0.26)
	Average	0.33	0.41	≥ 1.0	0.29	0.24
2.5F catheter	**1**	≥ 1.0	0.32 (0.26 – 0.37)	≥ 1.0	≥ 1.0	≥ 1.0
	2	≥ 1.0	0.34 (0.27 – 0.41)	≥ 1.0	≥ 1.0	≥ 1.0
	3	≥ 1.0	0.43 (0.32 – 0.54)	≥ 1.0	≥ 1.0	≥ 1.0
	Average	≥ 1.0	0.36	≥ 1.0	≥ 1.0	≥ 1.0
24G cannula + extension line	**1**	0.51 (0.47 – 0.54)	0.34 (0.32 – 0.35)	≥ 1.0	0.45 (0.42 – 0.50)	0.54 (0.49 – 0.57)
	2	0.43 (0.40 – 0.49)	0.45 (0.37 – 0.58)	≥ 1.0	0.48 (0.42 – 0.52)	0.51 (0.50 – 0.51)
	3	0.43 (0.42 – 0.44)	0.54 (0.51 – 0.55)	≥ 1.0	0.43 (0.42 – 0.44)	0.49 (0.47 – 0.50)
	Average	0.46	0.44	≥ 1.0	0.45	0.51

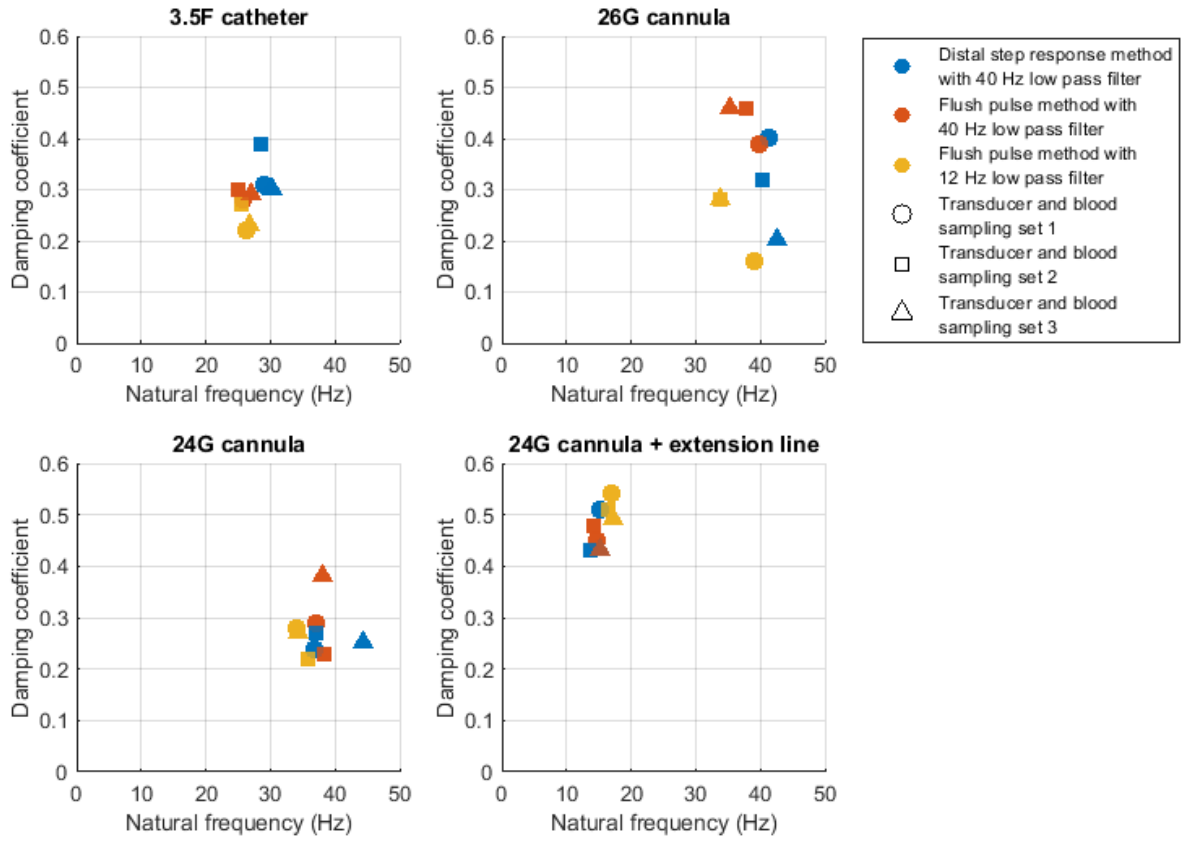

Figure 3.6: In-vitro measured dynamic response characteristics for four different types of catheters and three different transducer and blood sampling sets, using three different response methods. The average values of three consecutive measurements are shown.

The measured DR characteristics of one CMS prior to injection of a small air bubble, with an air bubble injected in the system, and after removal of the air bubble are shown in Tables 3.3 and 3.4, respectively. The average values are also visualized in Figure 3.7. When the air bubble was visible in the transducer dome, the natural frequency measured with the distal step response method more than halved and the damping coefficient increased. When the air bubble was visible in the blood sampling port, the natural frequency slightly increased again, while the damping coefficient further increased. After removal of the air bubble, the DR characteristics were comparable to those measured before injection of the air bubble using the distal step response method. Figure 3.7 also shows that when an air bubble was visible in the transducer dome, the DR characteristics measured using the proximal step response method were comparable to those measured with the distal step response method.

Table 3.3: Influence of a visible air bubble on the in-vitro measured natural frequencies using different response methods. Mean (minimal - maximal) values of three consecutive measurements are shown.

Catheter Manometer System	Natural frequency (Hz)		
	Distal step response method	Proximal step response method	Flush pulse method
Without air bubble	44.7 (42.9 – 46.8)	122.1 (114.8 – 133.8)	42.3 (41.0 – 44.0)
Air bubble in transducer dome	15.4 (15.3 – 15.5)	14.7 (14.3 – 15.3)	14.8 (14.8 – 14.9)
Air bubble in blood sampling port	26.9 (26.2 – 28.1)	78.2 (77.7 – 78.8)	19.2 (18.0 – 20.4)
Air bubble removed	39.1 (38.2 – 40.0)	95.1 (94.7 – 95.4)	37.1 (36.2 – 38.0)

Table 3.4: Influence of a visible air bubble on the in-vitro measured damping coefficients using different response methods. Mean (minimal - maximal) values of three consecutive measurements are shown.

Catheter Manometer System	Damping coefficient		
	Distal step response method	Proximal step response method	Flush pulse method
Without air bubble	0.27 (0.24 – 0.30)	0.33 (0.26 – 0.37)	0.33 (0.31 – 0.35)
Air bubble in transducer dome	0.42 (0.39 – 0.44)	0.45 (0.37 – 0.52)	0.41 (0.40 – 0.42)
Air bubble in blood sampling port	0.51 (0.44 – 0.61)	0.17 (0.15 – 0.18)	0.46 (0.43 – 0.50)
Air bubble removed	0.23 (0.21 – 0.25)	0.15 (0.14 – 0.17)	0.31 (0.21 – 0.37)

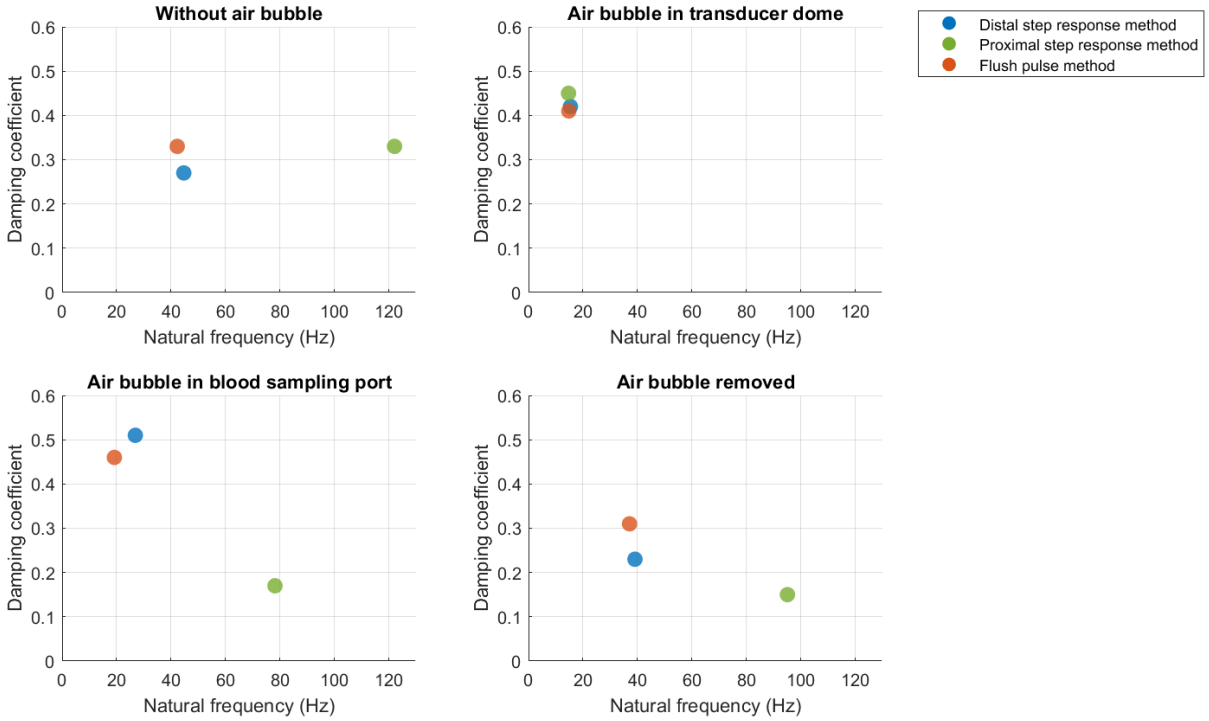

Figure 3.7: The influence of a visible air bubble on the in-vitro measured dynamic response characteristics using three different response methods. The average values of three consecutive measurements are shown.

3.4 Discussion

3.4.1 Comparison of the Proximal Step Response and Flush Pulse Method with the Distal Step Response Method

This in-vitro study showed that the DR characteristics measured with the flush pulse method are comparable to those measured with the distal step response method, while the proximal step response method considerably overestimates the natural frequency. An explanation for this is that the proximal step response method does not activate the whole CMS, since the response is generated in the compartment between the flush valve and the three-way stopcock (the red stopcock in Figure 3.1). Prior to the response, when the stopcock is closed to the transducer, a pressure difference occurs over this stopcock as the flow rate of the infusion pump is briefly increased. After this stopcock is turned towards the syringe, the closed flush valve presumably acts as the main resistance to the flow of saline towards the distal end of the catheter. This leads to a pressure difference over the flush valve. Therefore, a step response is elicited in the compartment between the flush valve and the stopcock, but not in the rest of the tubing. This is supported by the findings that adding an extension line had no influence on the measured DR characteristics using the proximal step response method, while a visible air bubble in the transducer dome did.

The flush pulse method also generates a response near the transducer. However, the impulse response seems to activate the transducer as well as the whole CMS, as is observed during the fast flush test [50]. When using the 40 Hz low pass monitor filter, a small amplitude, high frequency oscillation was visible on top of the larger amplitude, lower frequency oscillation (see Figure 3.5). This high frequency oscillation was previously observed during the fast flush test too and assumed to be caused by the transducer response [50, 51]. Another source might be the amplification of noise after taking the first derivative of the signal. However, this cannot explain why the high-frequency oscillation disappears at the end of the flush pulse. Regardless of whether the high-frequency oscillation is caused by the transducer response or amplification of noise, it is reduced by the filtering and limited sampling frequency.

The results obtained with the flush pulse method were comparable to those obtained with the distal step response method, especially for situations in which the natural frequency was decreased. The larger difference between the methods in case of higher natural frequencies was also observed by Van Langen et al. and can be explained by the influence of the monitor low pass filter [20]. Compared to a cut-off frequency of 12 Hz, a cut-off frequency of 40 Hz led to smaller average differences in the measured dynamic response characteristics between the flush pulse method and distal step response method. These differences were still larger than found by van Langen et al. [20], who calculated the average values of ten repeated measurements instead of three. Despite the observed differences, the flush pulse method is considered adequate for providing insights into the DR characteristics of CMS currently used in neonatal intensive care. Besides, the flush pulse method may approach the distal step response even more than the fast flush test that is used in adults, because there is no release of volumetric flow [49].

3.4.2 The Influence of Different Catheter Manometer System Configurations and Air Bubbles on the Dynamic Response Characteristics

The DR characteristics measured with the 24G and 26G cannulas were comparable. According to Equations 2.5 and 2.6, a smaller diameter of the cannula would decrease the natural frequency and increase the damping coefficient of the CMS, with a larger influence on the damping coefficient than on the natural frequency. The results of this study indeed suggest a slightly increased damping coefficient when using the smaller 26G cannula compared to the larger 24G cannula, but no clear difference in natural frequency. This might be explained by the fact that the diameter of only a small

fraction of the total length of the tubing was decreased. Furthermore, these results are in line with the results obtained from a randomized controlled trial evaluating the DR characteristics according to the cannula diameter used in adults [47]. In that study, the average natural frequency and damping coefficient were respectively 10.4 Hz and 0.26 measured with a 22G cannula and 10.5 Hz and 0.31 measured with a 24G cannula. The lower natural frequency compared to this study might be explained by the use of a different transducer and tubing set and because the results were obtained in-vivo instead of in-vitro. The natural frequencies measured in our study are in the range of the results obtained with a neonatal CMS and a 24G cannula in an in-vitro study by Van Langen et al. [20].
The natural frequency measured with the 3.5F catheter was lower compared to those measured with 24G and 26G cannulas, whereas the damping coefficient was slightly increased. This is as expected, since the length of the total tubing increased. Usage of the shorter, but smaller 2.5F catheter led to a damping coefficient ≥ 1.0.
Using an extra extension line of 200 cm more than doubled the total length of the CMS. Based on Equations 2.5 and 2.6, it was expected that the natural frequency would decrease and the damping coefficient would increase with a factor of approximately 1.5. However, the natural frequency was more than halved, while the damping coefficient was almost doubled. The larger decrease in natural frequency and increase in damping coefficient can be explained by the fact that the average radius of the total tubing also decreased by adding the extension line. Besides, Equations 2.5 and 2.6 are based on a model of the CMS that is a simplified representation of the actual CMS. Finally, the presence of an air bubble in the CMS also decreased the natural frequency and increased the damping coefficient, as described in literature [19, 51, 52].

3.4.3 Limitations and Recommendations

Validating the proximal step response and flush pulse method required a reliable reference method for determining the DR characteristics of CMS. The experimental setup used in this study for generating a distal step response resembles the classical pop or square wave test, which is commonly used to assess the dynamical properties of pressure monitoring systems [49, 53]. However, the DR characteristics were determined based on the assumption that the whole CMS can be modelled as an underdamped second-order dynamic system. It was previously suggested that after adding a catheter to the transducer and tubing set, the whole CMS should be modelled as a third order dynamic system [53]. However, based on the goodness of the fit shown in Figure 3.3, the assumption of a second-order dynamic system seems adequate for the CMS used in this study. Nevertheless, this assumption may be violated in case of an air bubble in the system [49].
Another assumption was that the monitor filter is a second-order Butterworth filter, as is commonly applied in monitoring devices [54]. The larger variance in measured DR characteristics for higher natural frequencies, when the low pass filter had a larger influence on the measured response, indicates that this assumption might be wrong. It is recommended to try to acquire information about the type of monitor filter that is used, in which we were unsuccessful, and eventually adjust Equation 3.1 accordingly.
Furthermore, while the results of this study suggested that the flush pulse method activates the whole CMS, this was not verified. This could be done by measuring the pressure at the catheter or cannula tip during the flush pulse test with a transducer tipped catheter, as previously performed during the fast flush test [50].
Lastly, the influence of different CMS configurations on the DR characteristics was studied in-vitro. When using the same catheter or cannula in-vivo, this may lead to different DR characteristics due to interaction with the patient's arterial system or an increased amount of air or blood in the CMS [19, 20, 53]. Therefore, it is recommended to assess the DR characteristics of CMS in-vivo using the flush pulse test to evaluate the accuracy of ABPW measurement in neonatal intensive care.

3.4.4 Clinical Implications

This study showed that the flush pulse method can be used to provide insights into the DR characteristics of CMS currently used at the NICU. Although there were still some small differences between the flush pulse method and the distal step response, these differences were smaller in cases of decreased natural frequency. In those situations, it is more important to measure the DR characteristics accurately, since this might enable the measurement-specific reconstruction of distorted ABPW [21, 22].

Unfortunately, the flush pulse method is, in contrast to the proximal step response method, not performed during routine interventions at the NICU. However, it is expected that this method can be easily implemented into clinical practice. Currently, the cut-off frequency of the monitor is set to 12 Hz. Due to the slightly increased difference between the flush pulse method and the distal step response method while using this cut-off frequency, it is recommended to set the cut-off frequency to 40 Hz while executing the flush pulse method. Repeating the flush pulse method more than three times may increase the accuracy of the measured DR characteristics.

The results of this study also indicate that a 2.5F catheter is not suitable for accurate ABPW measurement, due the overdamped response. Furthermore, the use of an extension line and presence of air bubbles worsen the DR characteristics of CMS. Therefore, it is recommended to limit the use of extension lines when possible and avoid air bubbles by carefully filling the CMS. Visible air bubbles in the transducer dome could be removed via the zeroing stopcock. Air bubbles that are introduced in the blood sampling port during blood sampling could only be removed by replacing the transducer and blood sampling set.

For advanced ABPW analysis in neonates, up to the tenth harmonic of the fundamental frequency of the signal should be preserved [46]. This means that the magnitude response of the monitoring chain should be close to one for frequencies up to 30 Hz. With a natural frequency around 40 Hz and a damping coefficient around 0.3, the magnitude response is increased to 1.6 for a frequency of 30 Hz (see Figure 3.8). This means that the higher harmonics in the ABPW signal are enhanced, resulting in a slightly underdamped signal. However, the monitor low pass filter will limit the enhancement. Figure 3.8 shows that the CMS in combination with a monitor filter cut-off frequency of 12 Hz, which is standardly used at the NICU, even leads to a reduction of the higher harmonics in the ABPW. When using a cut-off frequency of 40 Hz, the higher harmonics are still enhanced. Therefore, in both situations, the total monitoring chain does not give a flat frequency response up to 30 Hz. However, based on the results of this in-vitro study it is not possible to reach a conclusion on how the ABPW is affected by the monitoring system, because that should be based on the in-vivo measured DR characteristics at the NICU.

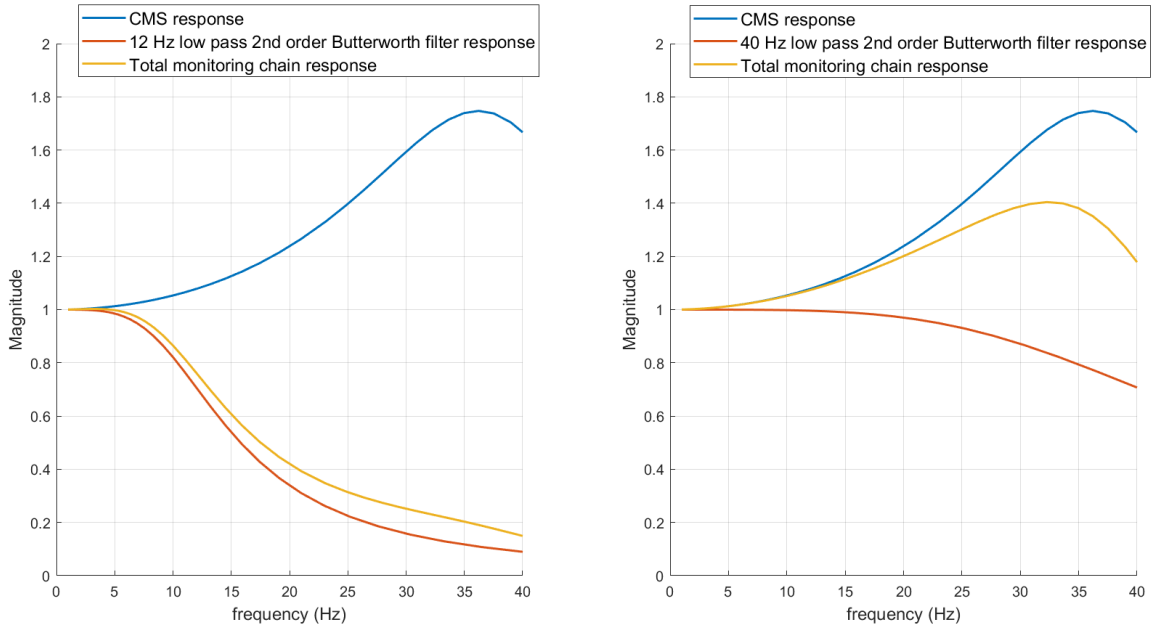

Figure 3.8: Magnitude response of the catheter manometer system, monitor low pass filter and total monitoring chain for a monitor filter cut-off frequency of 12 Hz (left) and 40 Hz (right).

3.5 Conclusion

This in-vitro study showed that the flush pulse method is comparable to the distal step response method for measuring DR characteristics of CMS used at the NICU, while the proximal step response method is not. Furthermore, it was shown that the addition of an extension line and presence of air bubbles in the CMS decreases its natural frequency and increases its damping coefficient. It is recommended to use the flush pulse method with a monitor filter cut-off frequency of 40 Hz for the in-vivo assessment of the DR characteristics of CMS at the NICU.

4 Accuracy of the Arterial Blood Pressure Waveform measured in Neonatal Intensive Care based on Dynamic Response Characteristics of Liquid-Filled Catheter Manometer Systems

4.1 Introduction

Accuracy of the measured arterial blood pressure waveform (ABPW) in neonatal intensive care depends on the dynamic response (DR) characteristics of liquid-filled catheter manometer systems (CMS) [17]. In the previous chapter, the in-vitro measured DR characteristics of these systems were described. However, the in-vivo DR characteristics of the CMS currently used at the neonatal intensive care unit (NICU) remain unknown. They may differ from the in-vitro measured characteristics due to interaction with the patient's arterial system or an increased amount of air or blood in the CMS [20, 53]. The in-vivo DR characteristics of CMS at the NICU can be assessed using the flush pulse test described by Van Langen et al. [20], which was validated in the previous chapter.

Based on the in-vivo measured DR characteristics, the effect of the CMS on the measured neonatal ABPW could be evaluated. Devasahayam et al. determined the errors in systolic, diastolic and mean pressures using simulated ABPW and a CMS with varying natural frequency and damping coefficient [55]. However, the simulated ABPW were based on the heart rates and blood pressure levels common in adults. Due to higher heart rates and lower pressure levels in the neonatal population, the measurement errors may be different. Van Genderingen et al. constructed iso-error curves for systolic, diastolic and pulse pressures measured in neonates, based on high-fidelity blood pressure recordings and a simulated CMS [17]. However, they did not consider the effect of the monitor low pass filter on the ABPW in addition to the CMS. This limits the clinical usefulness of these iso-error curves. Furthermore, the accuracy of other neonatal ABPW parameters, such as the systolic area under the curve (AUC) and the maximal slope of the upstroke (dP/dt), remains unknown. Information about the accuracy of these parameters is important for investigation or implementation of advanced ABPW analysis techniques, such as the Pressure Recording Analytical Method (PRAM) that uses the systolic AUC for estimation of the cardiac output [56, 57].

Next to this, the variability of DR characteristics over time within the same arterial line should be studied. For the interpretation of changes in the measured ABPW, it is useful to know whether changes in DR characteristics occur gradually or are related to certain routine clinical procedures, such as blood sampling and the replacement of the transducer and blood sampling set. In current clinical practice, the transducer and blood sampling sets are replaced every 48 hours, so that residual blood or air bubbles in the tubing are removed. In the previous chapter it was observed that the presence of an air bubble decreases the natural frequency and increases the damping coefficient. Therefore, it is expected that after a set replacement, the natural frequency increases and the damping coefficient decreases.

In summary, the primary aim of this study is to obtain the in-vivo DR characteristics of CMS used at the NICU using the flush pulse method. The secondary aim is to evaluate the effect of the total monitoring chain, composed of a CMS and monitor filter, on measured ABPW parameters. The tertiary aim is to investigate the variability of DR characteristics over time within the same arterial line.

4.2 Methods and Materials

4.2.1 In-Vivo Measurement of Dynamic Response Characteristics

All patients admitted to the NICU at the Radboudumc Amalia Children's Hospital with an arterial line in situ between 21-11-2022 and 20-12-2022 and on 16-01-2023 were included in this study. Four different catheter types were used: a 24-gauge (24G) cannula (Vigmed, Helsingborg, Sweden), 26G

cannula (Vigmed, Helsingborg, Sweden), 3.5-french (3.5F) 40 cm long catheter (Vygon, Ecouen, France) and 2.5F 30 cm long catheter (Vygon, Ecouen, France). The only exclusion criterion was high-frequency oscillatory ventilation. The DR characteristics of each CMS were assessed once a day during the inclusion period. Based on the results described in the previous chapter, the DR characteristics were measured using the flush pulse method proposed by Van Langen et al. [20] with a monitor low pass filter cut-off frequency of 40 Hz. With this method, the flush valve of the disposable pressure transducer and blood sampling set (Safedraw™-P, Merit Medical™, Galway, Ireland), was briefly opened and then released, which elicited an impulse response superimposed on the ABPW. This was repeated several times, so that at least one impulse response was elicited during the diastolic downstroke, which reduces the distortion of the measured response caused by the underlying ABPW. The measured signals were extracted from the patient monitor (IntelliVue MX750, Philips Medical Systems, Cambridge, Massachusetts, United States) and collected in a data warehouse with a sampling frequency of 125 Hz. As described in the previous chapter, the natural frequency f_n and damping coefficient ζ can be derived from the first derivative of the flush pulses by fitting Equation 3.1. The analyses were performed with Matlab (MATLAB R2022a, The MathWorks, Inc., Natick, Massachusetts, United States).

4.2.2 Evaluation of the Effect of the Total Monitoring Chain on the Neonatal Arterial Blood Pressure Waveform

Computer simulations were performed to evaluate the effect of the total monitoring chain on the neonatal ABPW. The total monitoring chain, composed of a CMS and monitor low pass filter, is schematically shown Figure 4.1.

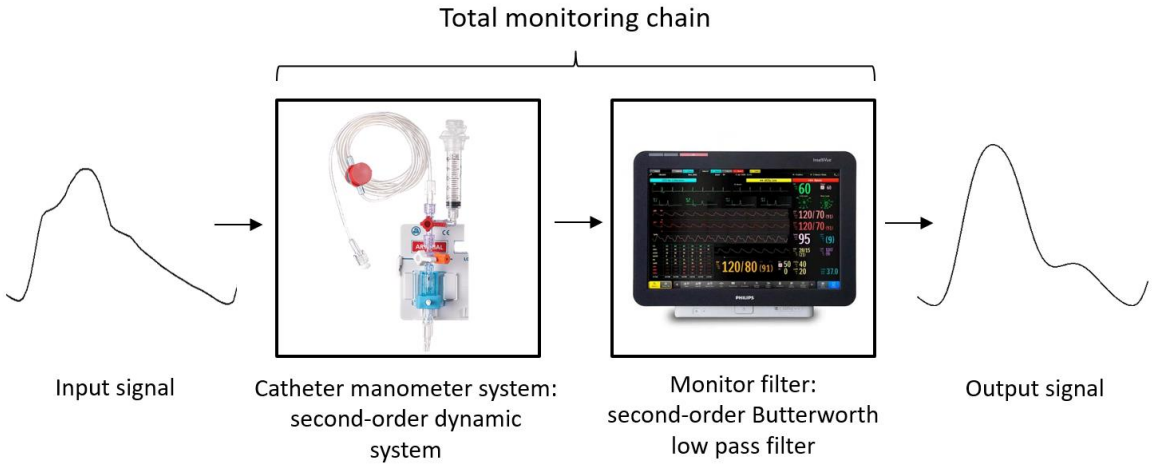

Figure 4.1: Schematic overview of the total monitoring chain for neonatal arterial blood pressure waveform measurement.

Figure 4.2 shows the characteristic neonatal ABPW that was used as the input signal, which was measured in the radial artery with a high-fidelity system by Gevers et al. [31]. The high-fidelity system was shown to have a natural frequency of 95 Hz and a damping coefficient of 0.15, resulting in a uniform frequency response up to 50 Hz. The signal was recorded with a monitor that was modified to pass higher harmonics up to 30 Hz and was sampled at 125 Hz. Up to ten harmonics of the fundamental frequency were visible in the amplitude spectrum of this signal (see Figure 2.4).

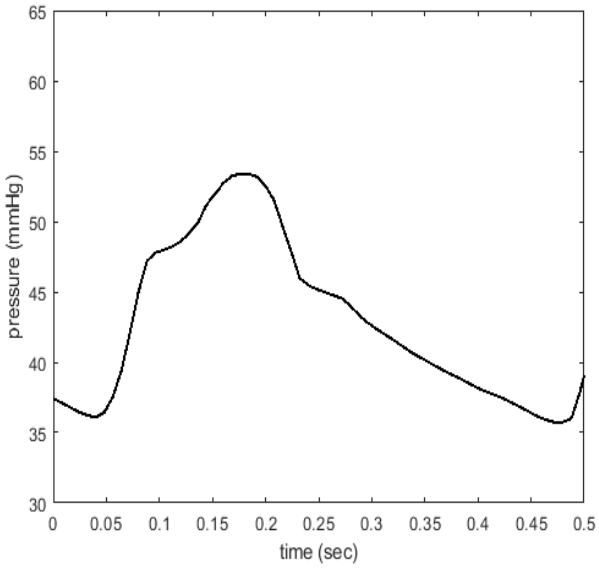

Figure 4.2: Characteristic neonatal arterial blood pressure waveform that was used as input signal, measured with a high-fidelity system and sampled at 125 Hz.

The input signal was passed through a CMS that was simulated as a second-order underdamped dynamic system, with the following transfer function (derived from Equation 2.4):

$$H_{CMS}(s) = \frac{\omega_n^2}{s^2 + 2\zeta\omega_n s + \omega_n^2}, \quad \text{(Eq. 4.1)}$$

where s is the Laplace operator, $\omega_n = 2\pi f$ the natural frequency in rad/s and ζ the damping coefficient. The natural frequency was varied from 5 to 40 Hz with increments of 1 Hz and the damping coefficient was varied from 0.1 to 0.8 with increments of 0.1. After passing the input signal through the simulated CMS, it was filtered with a second-order Butterworth low pass filter with a cut-off frequency of 12 Hz or 40 Hz. The resulting output signals were quantitatively compared to the input signal, by calculating the percentage error of the following parameters: mean, systolic, diastolic, pulse and dicrotic notch pressures, maximal dP/dt, total AUC, and systolic AUC. The calculation of these parameters is described in Appendix C. The simulations and analyses were performed with Matlab (MATLAB R2022a, The MathWorks, Inc., Natick, Massachusetts, United States).

4.2.3 Variability of DR characteristics over time

The variability of DR characteristics over time was studied in two patients that were hemodynamically stable and did not require frequent blood sampling. This facilitated the assessment of DR characteristics over time in a stable situation. Furthermore, the DR characteristics were determined prior to and after blood sampling and replacement of the transducer and blood sampling set. The effects of these routine clinical procedures on the measured ABPW were visualized. In one patient, the DR parameters were assessed prior to and after removal of the arterial line, so that the influence of the interaction of the patient's arterial system with the CMS could be studied.

4.3 Results

4.3.1 In-Vivo Measurement of Dynamic Response Characteristics

18 patients with 20 arterial lines in total were included in this study. The patient characteristics and arterial line characteristics are shown in Tables 4.1 and 4.2, respectively.

Table 4.1: Patient characteristics. N = sample size, n = number of patients. Female gender is reported as number (percentage). Gestational age and birth weight are reported as median (interquartile range).

	N=18
Female (n (%))	9 (50)
Gestational age (weeks $^{+\text{days}}$)	35^{+0} (28^{+3} – 37^{+4})
Birth weight (g)	1914 (1541 – 2890)

Table 4.2: Arterial line characteristics. N = sample size, n = number of arterial lines. Arterial line position and catheter type are reported as number (percentage). Number of measurements per arterial line and number of indwelling days at measurement are reported as median (interquartile range).

	N=20
Arterial line position (n (%))	
- **Radial artery**	7 (35)
- **Ulnar artery**	3 (15)
- **Dorsalis pedis artery**	3 (15)
- **Femoral artery**	1 (5)
- **Umbilical artery**	6 (30)
Catheter type (n (%))	
- **24G cannula**	13 (65)
- **26G cannula**	1 (5)
- **3.5F umbilical catheter**	5 (25)
- **2.5F umbilical catheter**	1 (5)
Number of measurements per arterial line	2 (1-4)
Number of indwelling days at measurement	3 (2-5)

Executing the flush pulse method once a day for all arterial lines during the inclusion period yielded 49 measurements, of which 48 are shown in Figure 4.3. The CMS with the 2.5F umbilical catheter did not show an oscillatory response and is therefore not indicated. Figure 4.3 shows that there is considerable variability in DR characteristics between different arterial lines, but also within the same arterial line. The median natural frequency of the 48 measurements was 15.5 Hz (interquartile range (IQR) 11.3 – 23.1 Hz) and the median damping coefficient was 0.29 (IQR 0.23 – 0.41). For 11 arterial lines, multiple measurements were performed. The median difference between the minimal and maximal natural frequency and damping coefficient measured with the same arterial line were respectively 11.6 Hz (IQR 4.4 – 19.3 Hz) and 0.18 (IQR 0.01 – 0.26). The lowest values of the natural frequency and damping coefficient were measured with a 3.5F umbilical catheter.

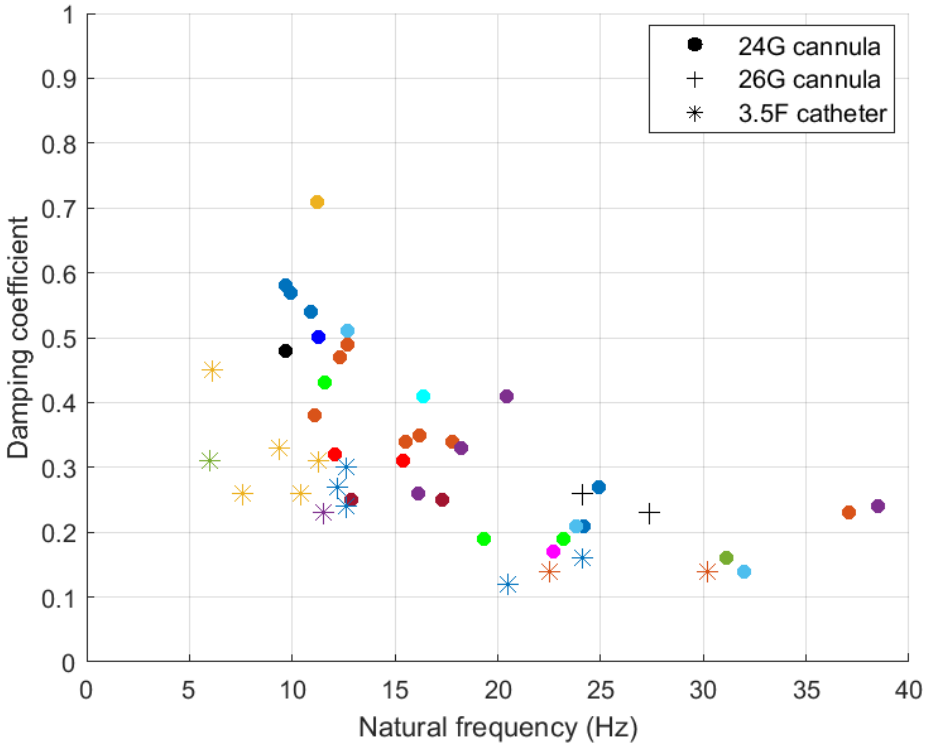

Figure 4.3: Measured dynamic response characteristics of catheter manometer systems at the neonatal intensive care unit using the flush pulse method. 48 measurement points of 19 arterial lines are shown. The catheter manometer system with the 2.5F catheter did not show an oscillatory response and is therefore not indicated. The other catheter types are indicated with different symbols, using different colors for the individual arterial lines.

4.3.2 Evaluation of the Effect of the Total Monitoring Chain on the Neonatal Arterial Blood Pressure Waveform

The effects of different DR characteristics of CMS in combination with a 40 Hz or 12 Hz monitor low pass filter on a characteristic neonatal ABPW are shown in Figures 4.4 and 4.5, respectively. Using the 40 Hz monitor low pass filter, the ABPW is mainly influenced by the CMS. Figure 4.4 shows that the errors in mean pressure, diastolic pressure and AUC are below 1%. The other ABPW parameters are more influenced by the DR of the CMS. The lower the natural frequency and damping coefficient, the larger the increase in systolic and pulse pressures and the larger the decrease in dicrotic notch pressure. Maximal dP/dt is increased with lower damping coefficients, while it is decreased with higher damping coefficients. The lower the natural frequency, the smaller the range of damping coefficients that result in accurate measurement of maximal dP/dt. Lastly, the systolic AUC is increased with lower natural frequencies. Based on the in-vivo measured DR characteristics of CMS and using a 40 Hz monitor low pass filter, the errors in pulse and dicrotic notch pressures, maximal dP/dt and systolic AUC of a characteristic neonatal ABPW exceed 10%. Figure 4.5 shows that the 12 Hz low pass monitor filter suppresses the increases in systolic and pulse pressures and decrease in dicrotic notch pressure. Although this filter also diminishes the increase in maximal dP/dt, it leads to a decrease in maximal dP/dt with almost all included CMS. There is also a larger increase in systolic AUC when using the 12 Hz filter compared to the 40 Hz filter.

Examples of output signals of the simulated CMS with several combinations of DR characteristics and the clinically used 12 Hz monitor low pass filter are shown in Figure 4.6. This figure shows that the lower the natural frequency, the more the output signal deviates from the input signal. The output signal appears overdamped in case of high damping coefficient and underdamped in case of low damping coefficient. If the natural frequency of the CMS is high, the output signal is still slightly overdamped due to the effect of the monitor low pass filter.

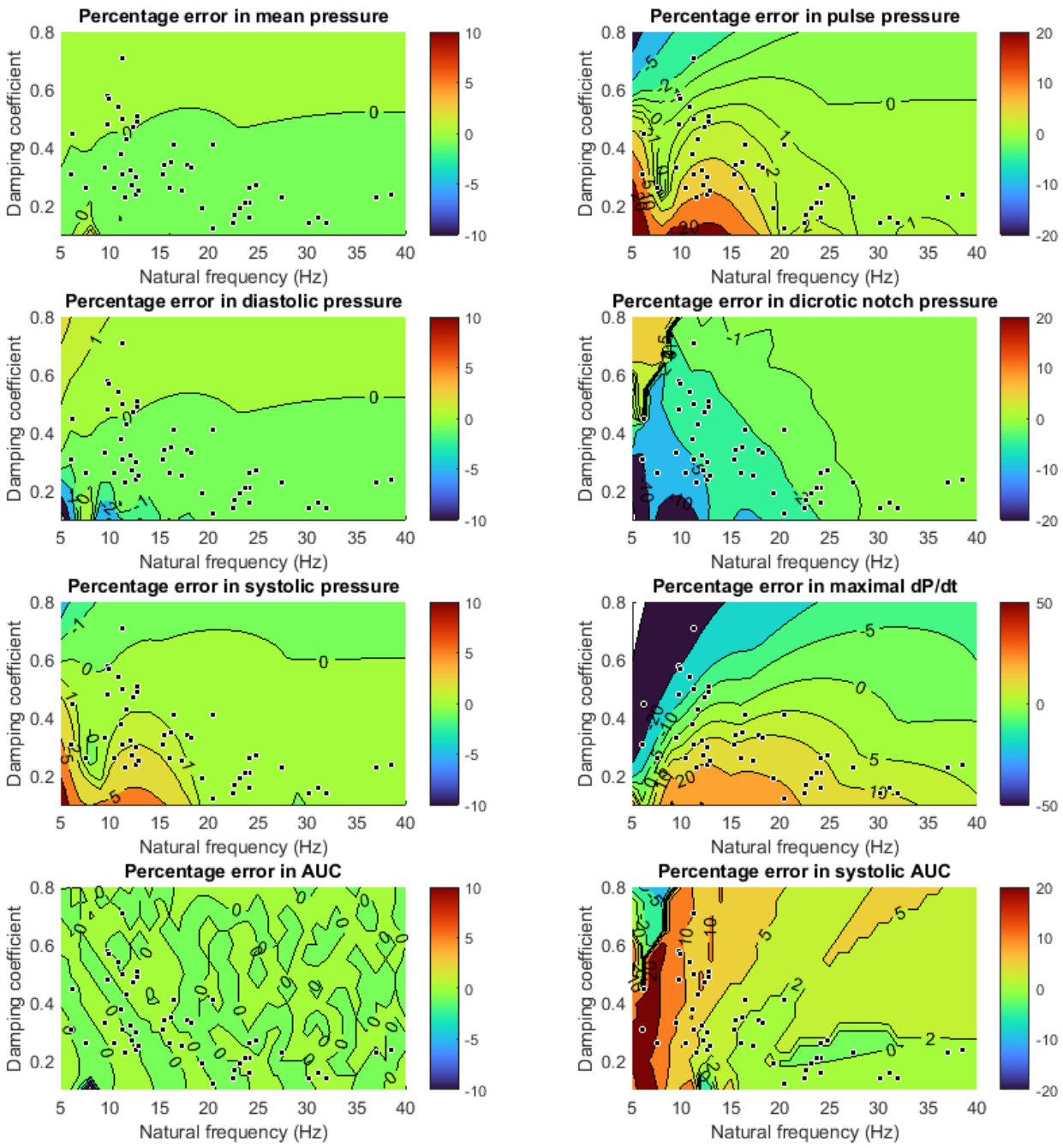

Figure 4.4: Percentage error in arterial blood pressure waveform parameters caused by the dynamic response of the catheter manometer system in combination with a 40 Hz monitor low pass filter. Individual measurement points of dynamic response characteristics are shown. The errors were calculated by quantitatively comparing the output signals, obtained after passing the high-fidelity input signal through a simulated monitoring chain, to the input signal. Note the different color-bar scales. AUC = area under the curve, dP/dt = slope of the systolic upstroke.

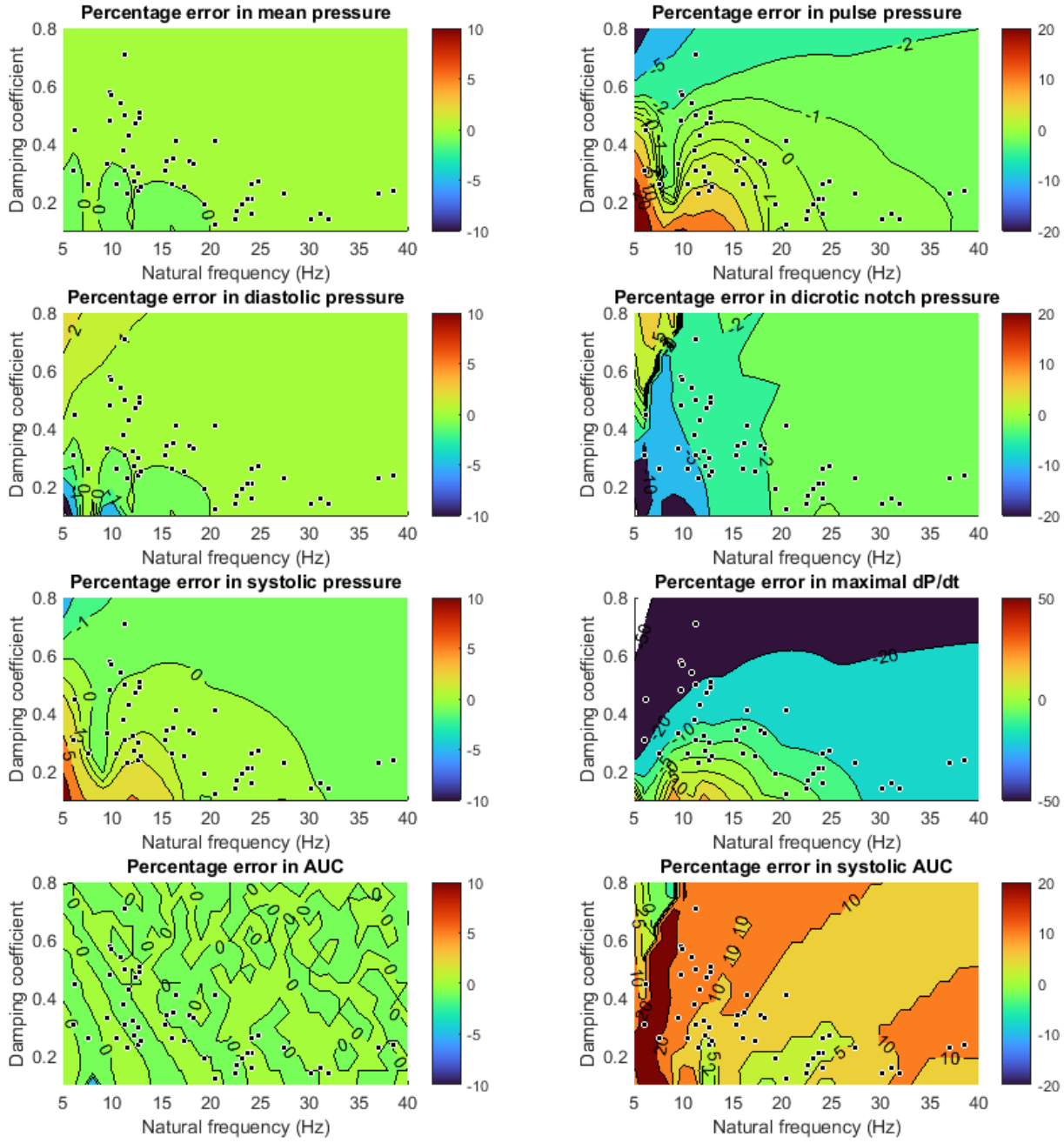

Figure 4.5: Percentage error in arterial blood pressure waveform parameters caused by the dynamic response of the catheter manometer system in combination with a 12 Hz monitor low pass filter. Individual measurement points of dynamic response characteristics are shown. The errors were calculated by quantitatively comparing the output signals, obtained after passing the high-fidelity input signal through a simulated monitoring chain, to the input signal. Note the different color-bar scales. AUC = area under the curve, dP/dt = slope of the systolic upstroke.

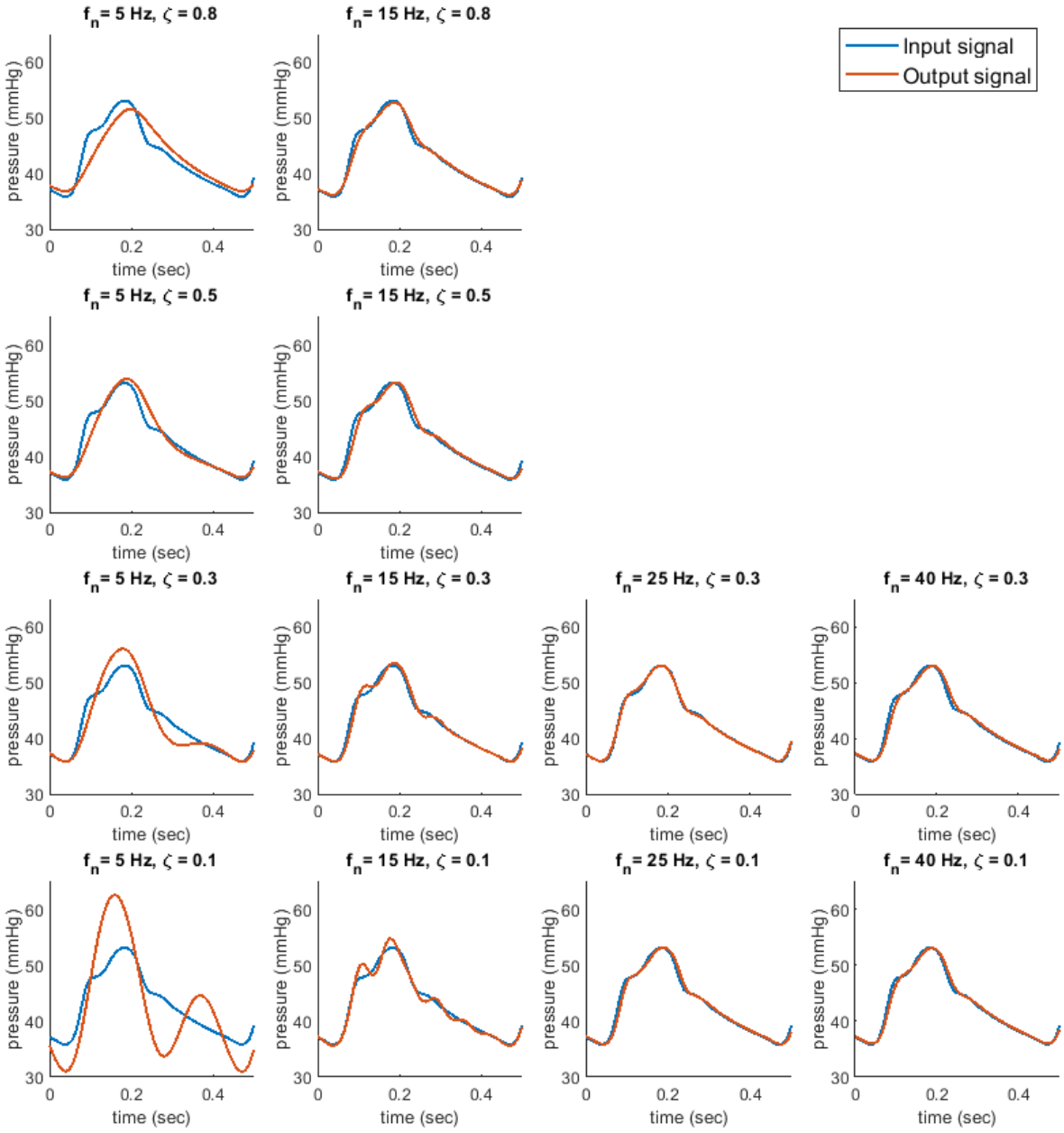

Figure 4.6: Examples of output signals after passing the high-fidelity input signal through simulated catheter manometer systems with several combinations of dynamic response characteristics and a 12 Hz monitor low pass filter.

4.3.3 Variability of Dynamic Response Characteristics over Time

The variability of DR characteristics over time in two patients is shown in Figure 4.7. Both patients had a 24G cannula in situ, in the radial artery in patient A and in the ulnar artery in patient B. In patient A, the measurements were started when the arterial line was 20 hours in situ, after an extra set replacement due to an obstruction alarm. The system was replaced again after 48 hours in situ following standard protocol. In patient B, the sets were replaced every 48 hours. Figure 4.7 shows that in patient A, the measured DR characteristics were close to each other after both system replacements and prior to the first blood sampling event after the replacements. After blood sampling, the natural frequency decreased and the damping coefficient increased. The first measurement performed after arterial line removal showed only a small change in DR characteristics. However, after flushing the line, the natural frequency increased and the damping coefficient decreased again. In patient B, the natural frequency changed less over time, but the damping coefficient increased after both set

replacements. The measured ABPW measured a few minutes before and after the different events in the two patients are shown in Figure 4.8. This figure shows that the waveforms measured in patient A hardly changed after each event, whereas the waveforms in patient B appeared overdamped after both set replacements.

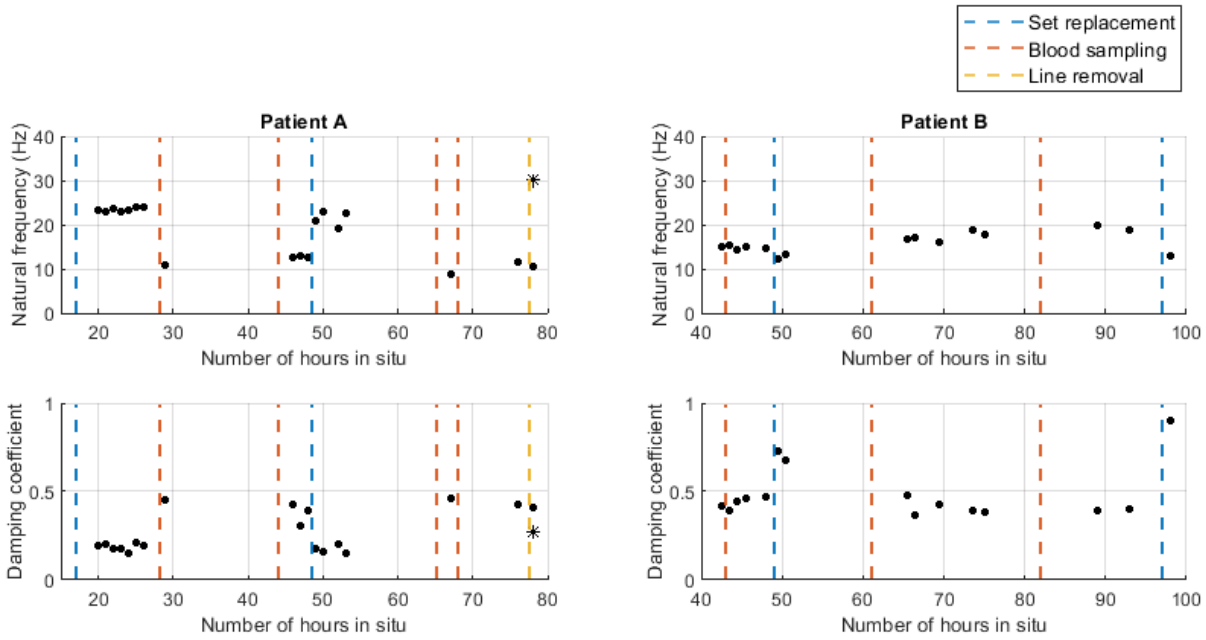

Figure 4.7: Natural frequency (top) and damping coefficient (bottom) measured over time in patient A (left) and B (right). Replacement of the transducer and blood sampling set, blood sampling and line removal are indicated with dotted lines. The asterisks indicate the values measured after flushing the catheter manometer system of patient A.

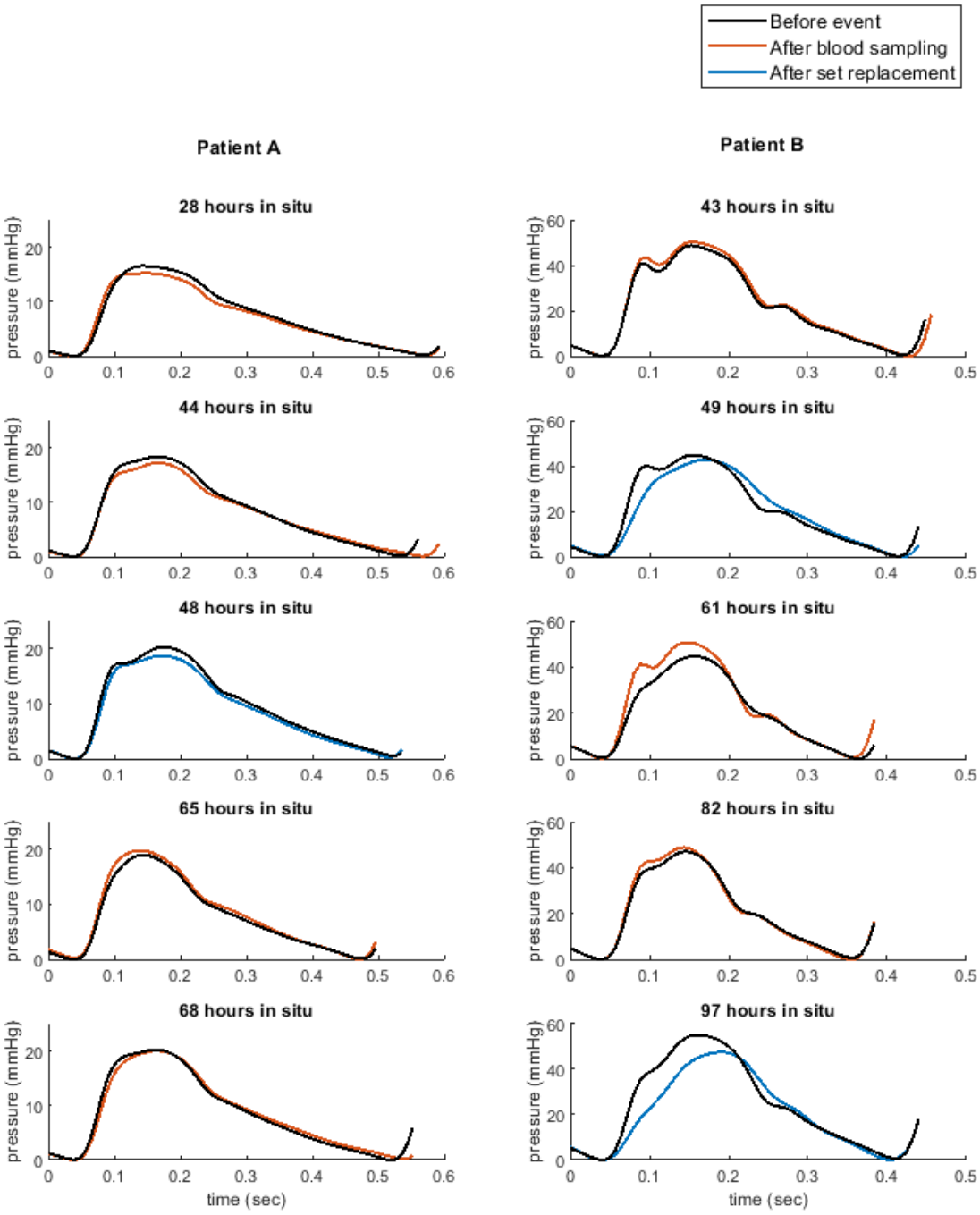

Figure 4.8: Measured arterial blood pressure waveforms in two patients before and after blood sampling and set replacement. A 12 Hz monitor low pass filter was used. Diastolic pressure was set to 0 mmHg.

4.4 Discussion

To our knowledge, this is the first study that evaluated the accuracy of the total ABPW monitoring chain used in neonatal intensive care, composed of a CMS and monitor low pass filter. The in-vivo measured DR characteristics showed that CMS at the NICU mainly cause underdamping of the ABPW, manifested as an increase in systolic and pulse pressures and maximal dP/dt. The 12 Hz monitor low pass filter suppresses the underdamping caused by the CMS for harmonics with a frequency above its cut-off frequency. The downside of using this filter is a decrease in maximal dP/dt and increase in systolic AUC. The latter can be explained by a right shift of the dicrotic notch, which is caused by the relative overdamping of the curve. The larger errors in several parameters around certain natural

frequencies and with low damping coefficients are caused by enhancement of the specific harmonic frequencies of the input signal. The same phenomenon was observed by Devasahayam et al. [55].
The in-vivo measured natural frequencies were in general lower than those measured in-vitro, whereas the in-vivo measured damping coefficients were comparable or higher. This corresponds to the findings by van Langen et al. [20]. The measured damping coefficients were similar to those measured previously in adults [47, 55]. The median natural frequency measured in this study was almost 8 Hz lower compared to the results of Devasahayam et al. [55], whereas it was 5 Hz higher than measured by Oh et al. [47]. The variability in measured natural frequencies might be explained by differences in the composition of transducer and blood sampling sets between different studies. For example, the inclusion of a blood-conserving device may decrease the natural frequency whithout affecting the damping coefficient [58].
In this study, it was shown that DR characteristics of CMS at the NICU could vary considerably, even within the same patient. Primarily the replacement of the transducer and blood sampling set and the first blood sampling event after replacement changed the DR characteristics in two patients. Therefore, the presence of residual blood and air bubbles in the CMS seem important factors that determine the DR characteristics. In one patient, the natural frequency increased and the damping coefficient decreased after a set replacement, as expected. However, in the other patient the damping coefficient increased after the set replacement. A possible explanation is that the new set was inaccurately filled with saline, thereby leaving an air bubble in the CMS. Air bubbles were occasionally seen in the blood sampling port, which could be introduced or removed by blood sampling. The interaction of the CMS with the patient's vasculature seems of less importance for the DR characteristics, since these hardly changed immediately after removal of the arterial line in patient A. This corresponds to the findings in adults by Kleinman et al [59]. The DR characteristics did change after the CMS was flushed, presumably because the residual blood from the distal part of the CMS was then removed too. After flushing the natural frequency and damping coefficient were comparable to those measured in-vitro with a 24G cannula (see previous chapter).
Although the measured ABPW after each set replacement and blood sampling event in patient B changed according to the measured DR characteristics, the ABPW measured in patient A hardly changed. It should be noted that the effect of certain DR characteristics depend on the original wave shape [55]. For example, the amplitude of higher harmonic frequencies depend on the prominence of anacrotic and dicrotic notches, which depends on the timing and magnitude of wave reflections [60]. Both the magnitude of wave reflections and the pulse pressure (PP) increase with aortic stiffness, suggesting that aortic stiffness of patient B was higher compared to patient A [35]. Because of these differences in waveforms, the simulated errors in ABPW parameters should be interpreted as possible errors in measured neonatal ABPW, but not as the actual errors. Furthermore, the previous chapter showed that the measured DR characteristics using the flush pulse method slightly differ from those measured using the distal step response method. However, these differences were small compared to the range of DR characteristics measured in this in-vivo study.

4.4.1 Limitations and Recommendations

This study has several limitations. First of all, only 20 indwelling arterial lines in a total of 18 patients were included. Although these 18 patients covered a range of gestational ages and birth weights, expanding the study population will provide a more comprehensive insight into the DR characteristics of CMS at the NICU. Furthermore, the variability of DR characteristics over time was studied in only two patients and the DR characteristics after line removal were assessed only once. The hypothesis that significant changes in DR characteristics only occur after replacement of the set and the first blood sampling event after replacement should be evaluated in the future.

Another important limitation is that the flush pulse method was not validated for the in-vivo measurement of DR characteristics. It was only validated in-vitro against a reference method in the previous chapter, when there was no interference of the underlying ABPW. The fact that repeated measurements of DR characteristics during a stable situation in two patients returned almost the same values suggests that the flush pulse method is precise. However, the in-vivo accuracy of the method was not demonstrated. It was previously shown in adults that the fast flush method is not affected by the underlying ABPW [59]. However, the diastolic portion of the ABPW in neonates is smaller than in adults, resulting in a smaller period when the blood pressure remains relatively constant. Furthermore, the CMS was assumed to be a second-order underdamped system and the monitor filter a second-order low pass Butterworth filter. It was previously stated that the CMS could be more accurately described by a third-order underdamped system [53]. The assumption of a linear underdamped system may also be violated in case of an air bubble in the CMS [49]. In spite of this, the model parameters were estimated from a measured response and these model parameters were subsequently used to evaluate the errors in measured ABPW parameters. Therefore, it is expected that the calculated errors in measured ABPW parameters are a reliable estimate of the possible errors measured in neonatal intensive care, although they were based on only one neonatal ABPW. It is straightforward that calculation of errors of other high-fidelity neonatal ABPW will give a more accurate estimate of the possible errors. The high-fidelity neonatal ABPW measured by Gevers et al. [61] could be used for this.

4.4.2 Clinical Implications

In current clinical practice, mean pressure and, to a lesser extent, PP are considered in the hemodynamic assessment of a neonate. This study showed that mean pressure is accurately measured by the total monitoring chain, regardless of the DR characteristics of CMS or the used monitor low pass filter. This is as expected, since both the CMS and monitor low pass filter were modelled as second-order dynamic systems, which preserve the zero frequency component of input signals. Errors in measured PP can be large, especially when using a 40 Hz monitor low pass filter. The clinically used 12 Hz monitor low pass filter suppresses the enhancement in PP caused by most CMS. However, with this filter the errors in PP could still vary between -5% and 10%. Therefore, this ABPW parameter should be interpreted with caution. Changes in PP might not only reflect changes in the cardiovascular status of the patient, but could also be caused by a change in DR characteristics of the CMS. The flush pulse method can be easily implemented into clinical practice to measure the DR characteristics of the CMS in situ, so that estimates of the errors in PP can be given.

As found in the previous chapter, this study showed that a 2.5F catheter is not suitable for accurate ABPW measurement, due the overdamped response. Current umbilical arterial catheter size recommendations vary based on institutional guidelines. While some guidelines recommend using a 2.5F catheter in neonates weighing less than 800-1000 g, others do not recommend using this catheter size at all [62]. The advantage of using a 2.5F over a 3.5F catheter in extremely low birth weight infants was not found in literature. Although a 2.5F catheter could still be used for measuring mean blood pressure, we recommended using a 3.5F catheter for more accurate measurement of PP in the umbilical artery. Figure 4.3 suggests that the 3.5F catheter causes more underdamping than the 24G and 26G cannulas. However, due to the small number of 3.5F catheters and 26G cannulas, it is not possible to draw any conclusion from these results. A lower natural frequency using a 3.5F catheter compared to a 24G or 26G cannula was also observed in-vitro, but no clear difference in damping coefficients was found (see Figure 3.6).

Besides the current clinical implications, the inaccuracy of the currently used monitoring chain limits the potential of advanced ABPW analysis for neonatal hemodynamic assessment. Since the errors in the measured systolic AUC can be as large as 20%, it is not recommended to implement any pulse

contour analysis technique with the currently used ABPW measurement method. Inaccuracy of the measured systolic AUC may also explain why PRAM differed significantly from the reference method is some studies, while in other studies acceptable performance was found [63]. Next to this, the possible errors in measured maximal dP/dt up to 20% may explain why using this parameter as a marker for cardiac contractility remains controversial [39].

To increase the accuracy of ABPW measurement in neonatal intensive care, the natural frequency of the CMS should be maintained as high as possible. Figure 4.4 shows that the errors in ABPW parameters are smaller over a wide range of damping coefficients in case of high natural frequency. Since the natural frequency decreased after blood sampling in one patient, using a separate arterial line for blood sampling will prevent this. However, inserting an extra arterial line is undesirable in all patients and especially in neonates, due to discomfort and risk of complications. Developing a double lumen arterial line seems a good alternative, but this will probably result in a decreased diameter of the tubing for pressure measurement, thereby decreasing the natural frequency and increasing the damping coefficient (see Equations 2.5 and 2.6). Furthermore, careful filling of each new set and removing visible air bubbles is important to prevent overdamping of the ABPW.

Another solution to increase the accuracy might be the measurement-specific reconstruction of distorted ABPW by taking the inverse of the transfer function of the total monitoring chain [21, 22]. Before implementation of this reconstruction method, it should be validated against a high-fidelity reference method. Several catheter-tip manometers exist with a flat frequency response over 1 kHz, meaning that these sensors do not distort the ABPW [64]. Unfortunately, these sensors are expensive and may break after only a few uses, further increasing its cost per use. A simpler option might be to compare the reconstructed ABPW just prior to and after set replacements, when the DR characteristics probably have changed. The reconstructed ABPW should be similar, because the ABPW is not expected to change over such a short time frame.

4.5 Conclusion

This study showed that the ABPW measured in critically ill neonates can be considerably affected by the DR characteristics of CMS in combination with a monitor low pass filter. The variation in DR characteristics across and within individual arterial lines suggests that the presence of air bubbles or blood are important factors that determine the DR. Neonatal ABPW parameters aside from the mean and diastolic blood pressures should be interpreted with caution, limiting the potential of advanced ABPW analysis techniques in neonatal intensive care.

5 Reconstruction of the Arterial Blood Pressure Waveform measured in Neonatal Intensive Care based on Dynamic Response Characteristics of Liquid-Filled Catheter Manometer Systems

5.1 Introduction

The arterial blood pressure waveform (ABPW) measured in critically ill neonates can be considerably affected by the dynamic response (DR) characteristics of catheter manometer systems (CMS) in combination with a monitor low pass filter. This limits the clinical implementation of pulse contour analysis techniques at the NICU as well as the development of novel algorithms for advanced ABPW analysis. A high-fidelity manometer tipped catheter (MTC) for blood pressure measurement is not suitable for clinical use, since blood sampling and infusion of heparinized saline via this catheter is not possible [46]. Gevers et al. combined an MTC with a CMS in a novel high-fidelity system for neonatal ABPW measurement, which facilitated blood sampling as well as flushing with heparinized saline [65]. Unfortunately, an MTC is expensive and may break after only a few uses, further increasing its cost per use. Therefore, improving the accuracy of neonatal ABPW measurement with the currently used CMS is desired.

In chapters 3 and 4, it was shown that careful filling of each transducer and blood sampling set and avoiding the use of 2.5F catheters is important to limit the amount of overdamping. It was previously shown that flushing with alcohol or carbon dioxide prior to the filling procedure or filling with degassed saline could improve the DR of neonatal CMS [66]. However, these methods required about five more minutes to fill the system and were not always successful. Furthermore, flushing with alcohol may be harmful in the neonatal population. To prevent underdamping of the ABPW, there is a commercially available damping device that increases the damping coefficient while maintaining the natural frequency [67]. However, the damping coefficients of different Resonance OverShoot Eliminator (ROSE) devices were found to cover a wide range of 0.19 to 1.20 [67]. Therefore, these devices may increase the errors in measured ABPW parameters and are not appropriate for use in clinical practice. Furthermore, as shown in chapter 4, considerable variation in the DR characteristics across and within individual arterial lines exists. Therefore, an adaptable method to improve the measured ABPW is necessary.

Devasahayam et al. proposed to add a measurement-specific compensation filter to improve the accuracy of measured ABPW in adults [55]. Based on the measured DR characteristics of the CMS, a second-order compensation filter was manually adjusted to obtain a cumulative frequency response that is nearly flat from 0 to 20 Hz. However, it is not possible to obtain a completely flat frequency response with this type of compensation filter. Lambermont et al. developed a reconstruction method based on the inverse of the transfer function of the CMS [21]. The natural frequency and damping coefficient of this transfer function were determined using the fast flush test. Comparison of the reconstructed ABPW to the high-fidelity ABPW that was simultaneously recorded using an MTC in a pig showed good agreement. Hazeleger et al. validated a similar reconstruction method for neonatal ABPW through computer simulations of a CMS [22]. However, accurate reconstruction of the distorted ABPW depends on accurate measurement of DR characteristics of the CMS in situ [55]. In chapter 3, the flush pulse method for determining the DR characteristics of CMS was validated in-vitro, but its accuracy in-vivo was not demonstrated. Furthermore, both Lambermont et al. and Hazeleger et al. did not incorporate a monitor low pass filter in the monitoring chain. For the clinical implementation of the reconstruction method, the transfer function of the total monitoring chain including the monitor low pass filter should be considered. Therefore, the aim of this study is to propose and initially validate

a measurement-specific reconstruction method for distorted ABPW measured in neonatal intensive care based on DR characteristics of the CMS in situ and the monitor low pass filter.
Based on the results described in the previous chapter, it is expected that the DR characteristics change after a transducer and blood sampling set replacement. The measured ABPW may change accordingly, whereas the original ABPW is expected not to change considerably in a short time frame. Comparison of the reconstructed waveforms before and after the set replacement will therefore yield some first insights into the validity of the reconstruction method.

5.2 Methods and Materials

Besides patients A and B that were described in the previous chapter, all patients admitted to the NICU at the Radboudumc Amalia Children's Hospital that received a new transducer and blood sampling set (Safedraw™-P, Merit Medical™, Galway, Ireland) between 25-01-2023 and 16-02-2022 were included in this study. Three types of catheters were used: a 24-gauge (24G) cannula (Vigmed, Helsingborg, Sweden), a 26G cannula (Vigmed, Helsingborg, Sweden), and a 3.5-french (3.5F) 40 cm long catheter (Vygon, Ecouen, France). The only exclusion criteria were high-frequency oscillatory ventilation and the use of a 2.5F umbilical catheter. The DR characteristics of each CMS were assessed before and after the set replacement. As described in the previous chapter, the DR characteristics were measured using the flush pulse method with a monitor low pass filter cut-off frequency of 40 Hz. The flush pulse method was executed several times, so that at least one impulse response was elicited during the diastolic downstroke. The measured signals were extracted from the patient monitor (IntelliVue MX750, Philips Medical Systems, Cambridge, Massachusetts, United States) and collected in a data warehouse with a sampling frequency of 125 Hz. As described in chapter 3, the natural frequency f_n and damping coefficient ζ were derived from the first derivative of the flush pulses by fitting Equation 3.1. Based on the calculated natural frequency and damping coefficient, the transfer function of the total monitoring chain can be obtained (see Appendix B for the derivation):

$$H_{total}(s) = \frac{\omega_n^2}{s^2 + 2\omega_n\zeta s + \omega_n^2} \cdot \frac{\omega_c^2}{s^2 + \sqrt{2}\omega_c s + \omega_c^2}, \quad \text{(Eq. 5.1)}$$

with $\omega_n = 2\pi f_n$ the natural frequency of the CMS in rad/s, ζ the damping coefficient of the CMS, ω_c the monitor low pass filter cut-off frequency in rad/s, and s the Laplace operator. In theory, the original ABPW can be reconstructed from the measured ABPW by taking the inverse of this transfer function. However, simply taking the inverse of Equation 5.1 yields an improper transfer function with infinite gain at large frequencies. To overcome this problem, the inverse of Equation 5.1 is multiplied with the transfer function of a fourth-order Butterworth low pass filter with a cut-off frequency of 11 times the heart rate of the neonate. This enabled reconstruction of the ABPW up to the tenth harmonic of the fundamental frequency, while amplification of noise is limited.
Within ten minutes before and after the set replacement, artefact-free segments of ten waveforms were manually selected, measured with a monitor low pass filter cut-off frequency of 40 and 12 Hz. From these four segments, wave onsets were detected as described in Appendix C and average measured and reconstructed ABPW were subsequently created. The average waveforms were normalized from 0 to 1 in both pressure and time and dicrotic notches were detected as described in Appendix C. The normalized measured waveforms before and after set replacement were compared by calculating the root mean square error (RMSE) and difference in dicrotic notch index (DNI). This was repeated for the normalized reconstructed waveforms. The analyses were performed with Matlab (MATLAB R2022a, The MathWorks, Inc., Natick, Massachusetts, United States).

5.3 Results

Nine patients with an arterial line in situ were included in this study, of whom the characteristics are shown in Table 5.1. The measured DR characteristics before and after the transducer and blood sampling set replacement are shown in Figure 5.1. An increase as well as decrease in natural frequency and damping coefficient were observed after replacement. In most cases, the damping coefficient increased when the natural frequency decreased and vice versa.

Table 5.1: Patient and arterial line characteristics. N = sample size, n = number of patients or arterial lines. Female gender, arterial line position and catheter type are reported as number (percentage). Gestational age and birth weight are reported as median (interquartile range).

	N=9
Female (n (%))	3 (33)
Gestational age (weeks $^{+\text{days}}$)	36 $^{+2}$ (28 $^{+6}$ – 37 $^{+6}$)
Birth weight (g)	2100 (720 – 3050)
Arterial line position and catheter type (n (%))	
- **Radial artery (24G)**	3 (33)
- **Ulnar artery (24G)**	1 (11)
- **Dorsalis pedis artery (24G)**	1 (11)
- **Posterior tibial artery (26G)**	1 (11)
- **Umbilical artery (3.5F)**	3 (33)

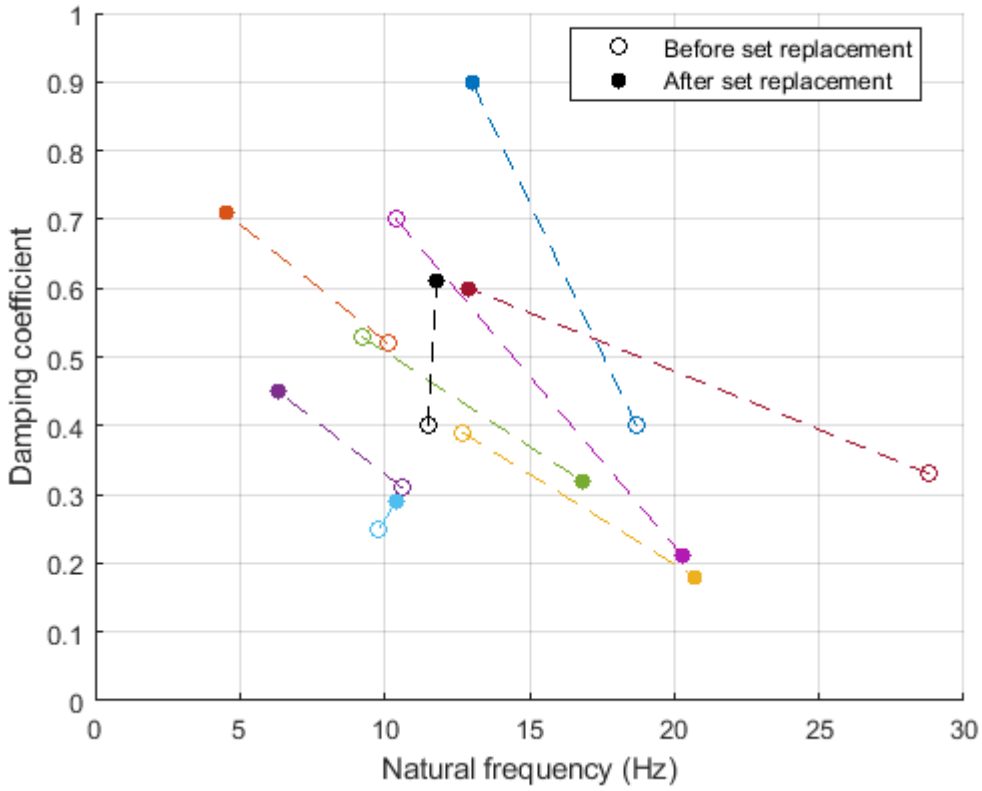

Figure 5.1: Change in measured dynamic response characteristics after the transducer and blood sampling set replacement in nine different patients, indicated by the different colors.

Figure 5.2 shows the RMSE and difference in DNI between measured as well as reconstructed ABPW before and after a transducer and blood sampling set replacement. The RMSE and difference in DNI

between measured ABPW was not in all patients related to the magnitude of change in DR characteristics. Using the 40 Hz monitor low pass filter, the difference in DNI between the ABPW decreased after reconstruction in six out of nine patients, while the RMSE decreased in only three patients. The median increase in RMSE and difference in DNI after reconstruction were respectively 0.01 (interquartile range (IQR) -0.01 – 0.06) and -0.02 (IQR -0.08 – 0.02). Using the 12 Hz monitor low pass filter, both the RMSE and difference in DNI decreased in only three patients after reconstruction. Using this filter, the median increase in RMSE and difference in DNI after reconstruction were respectively 0.02 (IQR -0.04 – 0.04) and 0.02 (IQR -0.07 – 0.15). The two patients in which a decrease respectively increase in RMSE and difference in DNI were found for both monitor filters, are shown in Figures 5.3 and 5.4. Although the reconstructed ABPW shown in Figure 5.3 were more similar than the measured ABPW, the reconstructed ABPW using the 40 Hz monitor low pass filter differed from the reconstructed ABPW using the 12 Hz monitor low pass filter. The four measured ABPW shown in Figure 5.4 have an overdamped appearance. While the reconstructed ABPW prior to the set replacement were similar to the measured ABPW, the reconstructed ABPW after set replacement differed considerably. Although the anacrotic notch became visible after the latter reconstruction, noise was amplified as well.

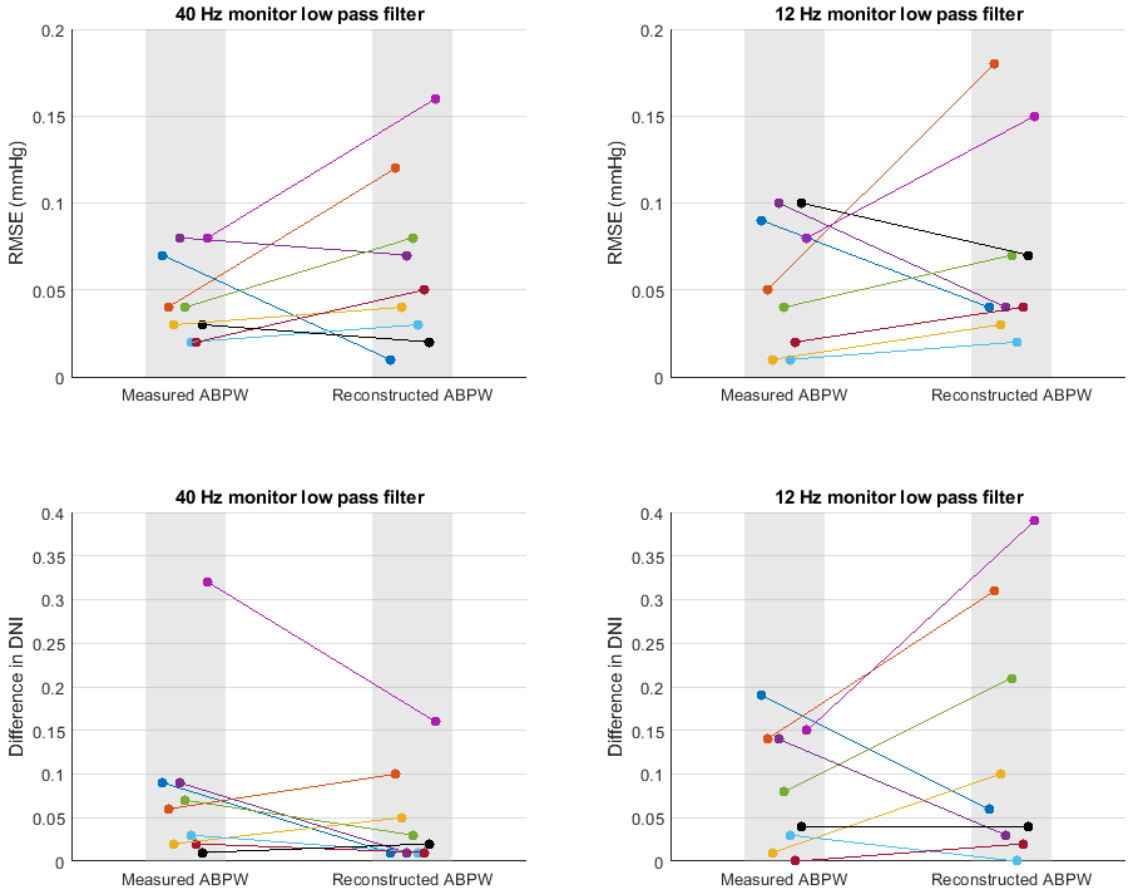

Figure 5.2: Comparison of measured as well as reconstructed arterial blood pressure waveforms before and after a transducer and blood sampling set replacement, using a 40 Hz monitor low pass filter (left) or a 12 Hz monitor low pass filter (right). ABPW = arterial blood pressure waveforms, DNI = dicrotic notch index, RMSE = root mean square error.

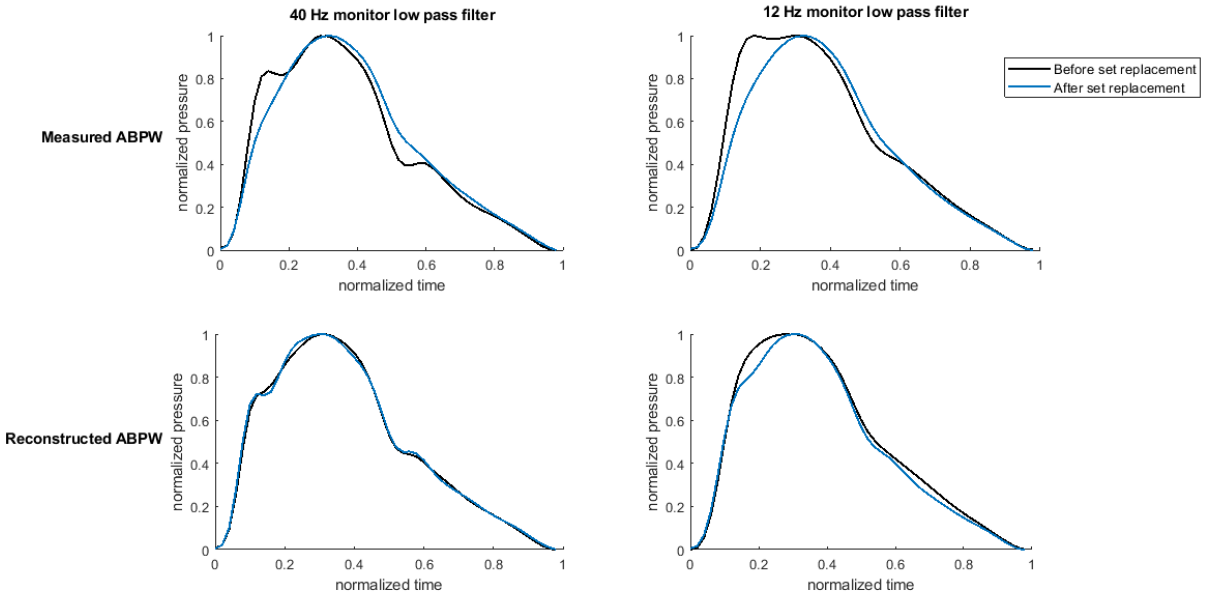

Figure 5.3: Examples of normalized measured (above) and reconstructed (below) arterial blood pressure waveforms (ABPW) before and after a transducer and blood sampling set replacement, using a 40 Hz (left) or 12 Hz (right) monitor low pass filter. The root mean square error and difference in dicrotic notch index decreased after reconstruction for both monitor filters.

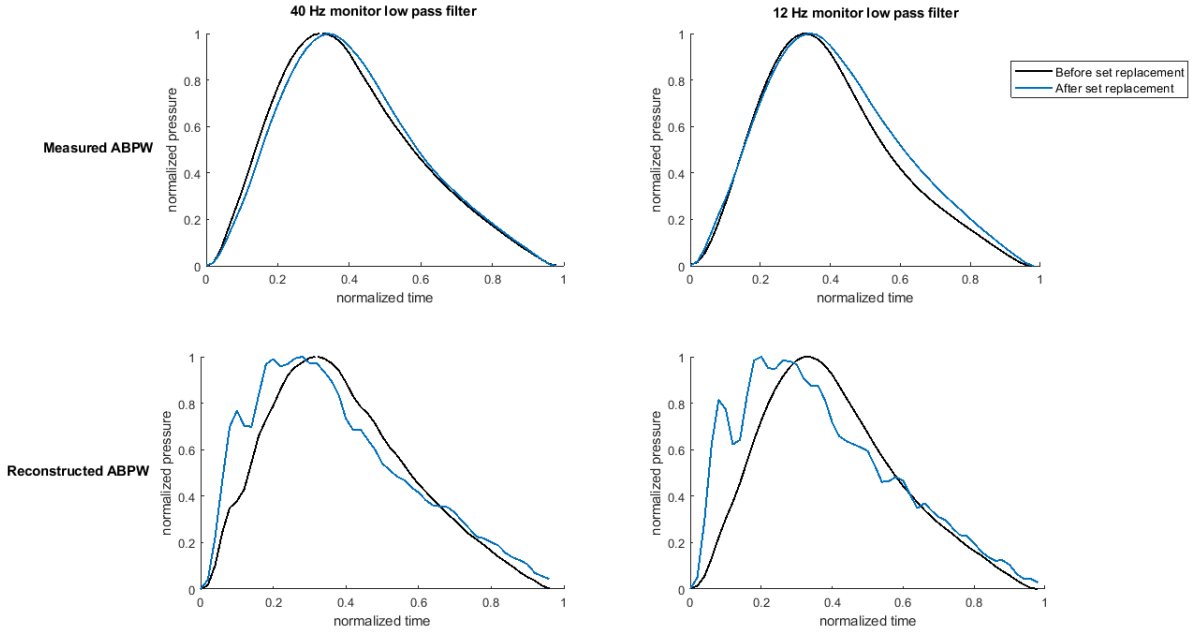

Figure 5.4: Examples of normalized measured (above) and reconstructed (below) arterial blood pressure waveforms (ABPW) before and after a transducer and blood sampling set replacement, using a 40 Hz (left) or 12 Hz (right) monitor low pass filter. The root mean square error and difference in dicrotic notch index increased after reconstruction for both monitor filters.

5.4 Discussion

In this study, a measurement-specific reconstruction method for distorted ABPW measured in neonatal intensive care was proposed based on measured DR characteristics of the CMS in situ and the monitor low pass filter. The results of this study suggest that the proposed reconstruction method

is not yet adequate for use in clinical practice and future research. Several explanations can be given for these results.

First of all, no high-fidelity APBW measurement method was used as reference for validation of the reconstruction method. Instead, the reconstructed ABPW before and after transducer and blood sampling set replacements were compared, based on the assumption that the actual ABPW were not altered in the small period of approximately ten minutes. However, changes in for example the heart rate were observed, which may have caused changes in the normalized ABPW due to a changed systolic to diastolic duration ratio. Furthermore, two similar reconstructed ABPW could still be different from the actual ABPW. As shown in Figure 5.3, the reconstructed ABPW using the 40 Hz monitor low pass filter differed from those using the 12 Hz monitor low pass filter. The reconstructed ABPW using the 40 Hz monitor low pass filter is presumably more accurate, since this filter does not modify the higher harmonics up to the at least the tenth harmonic frequency. Besides, the reconstructed ABPW using the 40 Hz monitor low pass filter shown in Figure 5.3 are similar to the high-fidelity neonatal ABPW measured by Gevers et al. [31].

Secondly, differences between the reconstructed ABPW before and after set replacement could have been caused by inaccurate assessment of the DR characteristics of the CMS in situ. The RMSE and difference in DNI between measured ABPW was not in all patients related to the magnitude of change in measured DR characteristics after set replacement. This might be explained by differences in the original ABPW as suggested in the previous chapter or due to the normalization. However, it may also indicate inaccurate measurement of DR characteristics. As stated before, the flush pulse method for assessing the DR characteristics of CMS was only validated in-vitro. It was shown that the average errors in measured natural frequency and damping coefficient were approximately 2.6 Hz and 0.7, respectively. However, the large amounts of air in the CMS that were occasionally observed in clinical practice (see Figure 5.5) may increase the errors in measured DR characteristics, because the assumption that the CMS can be modelled as a second-order dynamic system is probably violated in case of air in the liquid-filled catheter [49].

Thirdly, reconstruction of an overdamped waveform such as shown in Figure 5.4 is difficult due to the small amplitude of higher harmonics in the measured ABPW, especially when using a 12 Hz monitor filter. Because of the necessary large amplification of higher harmonics in the reconstruction, noise is amplified as well. Noise was also visible in the reconstructed ABPW of Lambermont et al. [21]. Averaging multiple reconstructed ABPW might decrease the extent to which noise is visible.

To prevent too much overdamping of the ABPW, careful filling and flushing to prevent air bubbles in the CMS is recommended. Furthermore, this may improve the accuracy of in-vivo assessment of DR characteristics, because the assumption that the CMS can be modelled as a second-order underdamped dynamic system is only true without air bubbles. In that case, the proposed reconstruction method might be more adequate. However, before this method can be implemented into clinical practice or future research, validation with a high-fidelity ABPW measurement system such as used by Gevers et al. [65] is required. Developing such a high-fidelity system will facilitate comparison of the ABPW measured with a CMS to the simultaneously measured high-fidelity ABPW. Besides, it enables in-vivo validation of the flush pulse method, since the DR characteristics can be obtained by comparing the frequency spectrum of the ABPW measured with the CMS with that of the high-fidelity ABPW [68].

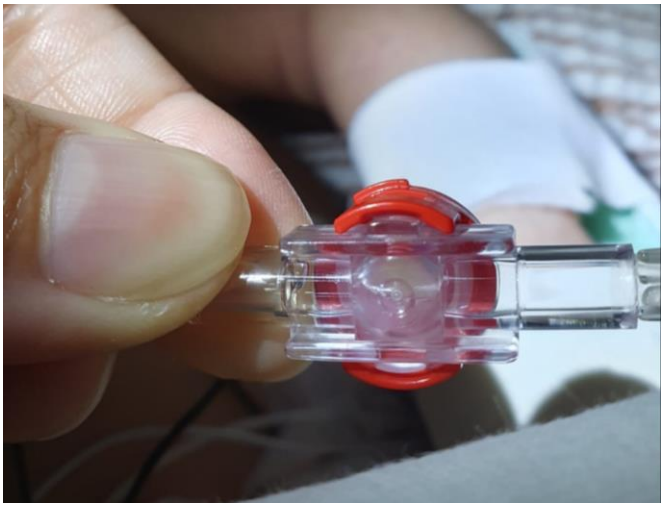

Figure 5.5: Visible air bubble in the blood sampling port of a catheter manometer system at the neonatal intensive care unit.

5.5 Conclusion

In this study, a measurement-specific reconstruction method for distorted ABPW measured in neonatal intensive care was proposed. Unfortunately, initial validation showed that this method is not yet adequate for use in clinical practice or future research. Careful filling and flushing of the CMS may improve both the accuracy of ABPW measurement and the proposed reconstruction method. Developing a high-fidelity ABPW measurement system will facilitate more accurate validation of this method.

6 Discussion

Advanced analysis of the arterial blood pressure waveform (ABPW), as part of comprehensive hemodynamic monitoring in critically ill neonates, requires an accurate measurement method. Measuring blood pressure with a liquid-filled catheter manometer system (CMS) is currently considered the gold standard in neonates [18]. However, the measured ABPW may be distorted by an inadequate dynamic response (DR) of the CMS [17]. The primary aim of this study was to evaluate the accuracy of the ABPW measured in neonatal intensive care based on DR characteristics of liquid-filled CMS.

In chapter 3, it was shown that the flush pulse method proposed by van Langen et al. [20] can be used to provide insights into the DR characteristics of CMS that are currently used in neonatal intensive care. In chapter 4, this method was applied to assess the in-vivo DR characteristics of CMS at the neonatal intensive care unit (NICU). These characteristics were similar to the previously in-vivo measured DR characteristics of CMS in adults [47, 55]. Computer simulations showed that the neonatal ABPW can be considerably affected by the DR of the CMS in combination with a monitor low pass filter. While mean pressure was not altered, pulse pressure (PP) increased and dicrotic notch pressure decreased due to underdamping by the CMS in most cases. The currently used 12 Hz monitor low pass filter suppresses the underdamping and is therefore recommended for clinical practice. However, considerable variation in DR characteristics across and within individual arterial lines was found, so that (changes in) PP should be interpreted with caution. In current clinical practice, the errors in PP could vary between -5% and 10%. Furthermore, the errors in the maximal slope of the systolic upstroke (dP/dt) and systolic area under the curve (AUC) as large as 20% limit the potential of advanced ABPW analysis techniques. Lastly, the results of this study imply that a CMS is not an ideal reference method for validation of novel noninvasive ABPW measurement methods, such as capacitive-based sensors [69].

To facilitate improvement of the accuracy of the measured ABPW in neonatal intensive care, possible causes of inadequate DR were identified. First of all, in chapters 3 and 4 it was shown that the 2.5F umbilical catheter is not suitable for ABPW measurement, due to the overdamped response. No clear difference in measurement accuracy between the other types of catheters was demonstrated. In chapter 3, it was shown that the presence of an air bubble in the CMS decreases its natural frequency and increases its damping coefficient, as described in literature [19, 51, 52]. The larger amount of air or blood in the CMS in clinical practice may explain why in-vivo measured natural frequencies were in general lower than those measured in-vitro, whereas the in-vivo measured damping coefficients were comparable or higher, corresponding to the findings by van Langen et al. [20]. Furthermore, it is plausible that the changes in measured DR characteristics after a transducer and blood sampling set replacement described in chapter 5 were caused by the introduction or removal of air bubbles or blood. Raising the awareness of health care personnel on the importance of careful filling and flushing of the CMS will hopefully reduce the variability in DR characteristics across and within individual arterial lines. Furthermore, without the presence of air bubbles in the CMS, the proposed measurement-specific reconstruction method may be more adequate.

6.1 Strengths and Limitations

To our knowledge, this is the first study that evaluated the accuracy of the total ABPW monitoring chain used in neonatal intensive care, composed of a CMS and monitor low pass filter. This yielded not only relevant information for current clinical practice, but also for the investigation or implementation of advanced ABPW analysis techniques. A strength of this study is that the method for assessing the DR characteristics of currently used CMS was first validated in-vitro by comparing it

to a reference method. Another strength is that the accuracy of neonatal ABPW measurement was evaluated based on in-vivo instead of in-vitro measured DR characteristics. By combining the in-vivo and in-vitro results, possible causes of inadequate DR were identified that may facilitate improvement of ABPW measurement. Lastly, a strength is that the initial validation of a measurement-specific reconstruction method was based on in-vivo measured DR characteristics and the corresponding measured ABPW, instead of computer simulations of the ABPW and monitoring chain.

Besides these strengths, this study has several limitations. First of all, only one type of transducer and blood sampling set was considered, limiting the generalizability of our results to other neonatal intensive care units (NICUs) that may use different sets. Next to this, the patient population that was included for the in-vivo assessment of DR characteristics of CMS was small and the variability of DR characteristics over time was assessed in only two patients. Besides, the effect of the total monitoring chain on the neonatal ABPW was evaluated based on assumptions about the behavior of the CMS and monitor low pass filter, and using only one high-fidelity neonatal ABPW. Although the measured ABPW in one patient changed as expected based on the measured DR characteristics, the ABPW in the other patient did not change. This can be explained by differences in the original ABPW, but also because of inaccurate assessment of DR characteristics. The flush pulse method was only validated in-vitro, because the reference method for assessment of DR characteristics cannot be applied in-vivo. This limits the use of the flush pulse method for accurate assessment of errors in measured ABPW parameters and accurate reconstruction of distorted ABPW.

6.2 Future Perspectives

First of all, raising the awareness of healthcare personnel on the importance of careful filling and flushing of the CMS with normal saline is important to prevent air bubbles in the CMS. To aid in this, a different design of the blood sampling port could be considered to reduce the chance of air bubble formation. As soon as the amount of air in the CMS is reduced in clinical practice, the flush pulse method should be validated in-vivo. It is recommended to develop a high-fidelity ABPW measurement system such as used by Gevers et al. [65] for this. Comparing the ABPW measured with a CMS to the simultaneously measured high-fidelity ABPW will not only provide an adequate validation method for the flush pulse method, but also provides the actual errors in measured ABPW parameters caused by the currently used monitoring chain as well as an adequate validation method for the proposed reconstruction method.

Until the accuracy of ABPW measurement in neonatal intensive care is improved or a valid reconstruction method exists, it is not recommended to investigate or implement any advanced neonatal ABPW analysis techniques as part of comprehensive hemodynamic monitoring. The use of other advanced cardiac output (CO) monitoring techniques have been proposed, such as electrical biosensing technologies and transpulmonary ultrasound dilution [12, 14]. Validation of these innovative techniques in the neonatal population is difficult, because the gold-standard method for CO assessment in the larger pediatric population, transpulmonary thermodilution, is not feasible in newborn infants due to size constraints [70]. The use of transthoracic echocardiography as a reference method is questionable due to the limited accuracy of this method, mainly related to the difficulty in measuring the cross-sectional area of the outflow tract, the angle between the blood flow direction and the ultrasound beam and the assumption of laminar flow [12]. Ultrafast vector flow imaging is a promising technique that might overcome these limitations [71]. Using this technique, the full 3-D cardiac blood flow patterns could be visualized. However, this technique is still in a research phase and requires high computational power, so that bedside assessment of CO is not yet possible.

Combining information about the CO with arterial oxygen saturation informs the clinician about global oxygen delivery in the neonate. However, it remains unknown whether oxygen delivery is sufficient

to meet oxygen demand, which is dependent on the level of basal metabolism, thermogenesis and external work [12]. Furthermore, a normal CO level does not guarantee adequate perfusion of all organs, such as the brain and intestines. Information about regional blood flow and tissue oxygenation and extraction may be obtained with near-infrared spectroscopy (NIRS). It was recently shown that combining NIRS with echocardiography and results from clinical assessment resulted in shorter recovery times in neonates with compromised hemodynamics [72]. Nevertheless, correct interpretation of all these measurements is important, for which knowledge about the pathophysiology of neonatal hemodynamics as well as the limitations of the used technology is essential. Therefore, expert consultation and extensive validation of advanced hemodynamic monitoring techniques is recommended.

6.3 Conclusion

Accuracy of the ABPW measured in critically ill neonates can be considerably affected by the DR of CMS in combination with the monitor low pass filter. While mean pressure is accurately measured, PP should be interpreted with caution in current clinical practice. Furthermore, the possibly large errors in measured maximal dP/dt and systolic AUC limit the potential of advanced ABPW analysis techniques. The variation in DR characteristics across and within individual arterial lines suggests that the presence of air bubbles or blood in the CMS are important factors that determine the DR. Careful filling and flushing of the CMS might improve the accuracy of ABPW measurement as well as assessment of DR characteristics, thereby improving the measurement-specific reconstruction method for distorted ABPW. Until the accuracy of ABPW measurement in neonatal intensive care is improved or a valid reconstruction method exists, it is not recommended to investigate or implement advanced ABPW analysis techniques as part of comprehensive neonatal hemodynamic monitoring.

References

[1] A. M. C. Watkins, C. R. West, and R. W. I. Cooke, "Blood pressure and cerebral haemorrhage and ischaemia in very low birthweight infants," *Early Human Development,* vol. 19, no. 2, pp. 103-110, 1989, doi: 10.1016/0378-3782(89)90120-5.

[2] K. Faust *et al.*, "Short-term outcome of very-low-birthweight infants with arterial hypotension in the first 24 h of life," *Archives of Disease in Childhood - Fetal and Neonatal Edition,* vol. 100, no. 5, p. F388, 2015, doi: 10.1136/archdischild-2014-306483.

[3] R. W. Hunt, N. Evans, I. Rieger, and M. Kluckow, "Low superior vena cava flow and neurodevelopment at 3 years in very preterm infants," *The Journal of Pediatrics,* vol. 145, no. 5, pp. 588-592, 2004, doi: 10.1016/j.jpeds.2004.06.056.

[4] S. E. Martens *et al.*, "Is hypotension a major risk factor for neurological morbidity at term age in very preterm infants?," *Early Human Development,* vol. 75, no. 1, pp. 79-89, 2003, doi: 10.1016/j.earlhumdev.2003.09.005.

[5] B. Batton *et al.*, "Blood Pressure, Anti-Hypotensive Therapy, and Neurodevelopment in Extremely Preterm Infants," *The Journal of Pediatrics,* vol. 154, no. 3, pp. 351-357.e1, 2009, doi: 10.1016/j.jpeds.2008.09.017.

[6] T.-W. Wu and S. Noori, "Recognition and management of neonatal hemodynamic compromise," *Pediatrics & Neonatology,* vol. 62, pp. S22-S29, 2021, doi: 10.1016/j.pedneo.2020.12.007.

[7] S. Noori and I. Seri, "Principles of Developmental Cardiovascular Phyisology and Pathophysiology," in *Hemodynamics and Cardiology: Neonatology Questions and Controversies*, I. Seri, M. Kluckow, and R. A. Polin Eds., 3 ed. Philadelphia, PA: Elsevier, Inc., 2019, ch. 1, pp. 3-27.

[8] S. Noori and I. Seri, "Evidence-based versus pathophysiology-based approach to diagnosis and treatment of neonatal cardiovascular compromise," *Seminars in Fetal and Neonatal Medicine,* vol. 20, no. 4, pp. 238-245, 2015, doi: 10.1016/j.siny.2015.03.005.

[9] W.-P. de Boode, "Clinical monitoring of systemic hemodynamics in critically ill newborns," *Early Human Development,* vol. 86, no. 3, pp. 137-141, 2010, doi: 10.1016/j.earlhumdev.2010.01.031.

[10] M. Laughon *et al.*, "Factors Associated With Treatment for Hypotension in Extremely Low Gestational Age Newborns During the First Postnatal Week," *Pediatrics,* vol. 119, no. 2, pp. 273-280, 2007, doi: 10.1542/peds.2006-1138.

[11] S. Noori and I. Seri, "Neonatal blood pressure support: the use of inotropes, lusitropes, and other vasopressor agents," (in eng), *Clinics in perinatology,* vol. 39, no. 1, pp. 221–238, 2012, doi: 10.1016/j.clp.2011.12.010.

[12] W.-P. de Boode, "Advanced Hemodynamic Monitoring in the Neonatal Intensive Care Unit," *Clinics in Perinatology,* vol. 47, no. 3, pp. 423-434, 2020, doi: 10.1016/j.clp.2020.05.001.

[13] C. E. Schwarz and E. M. Dempsey, "Management of Neonatal Hypotension and Shock," *Seminars in Fetal and Neonatal Medicine,* vol. 25, no. 5, p. 101121, 2020, doi: 10.1016/j.siny.2020.101121.

[14] S. L. Vrancken, A. F. van Heijst, and W. P. de Boode, "Neonatal Hemodynamics: From Developmental Physiology to Comprehensive Monitoring," *Frontiers in Pediatrics,* vol. 6, 2018, doi: 10.3389/fped.2018.00087.

[15] B. Saugel *et al.*, "Cardiac output estimation using pulse wave analysis—physiology, algorithms, and technologies: a narrative review," *British Journal of Anaesthesia,* vol. 126, no. 1, pp. 67-76, 2021, doi: 10.1016/j.bja.2020.09.049.

[16] J. Grensemann, F. Wappler, and S. G. Sakka, "Erroneous continuous cardiac output by calibrated pulse contour analysis," *Journal of Clinical Monitoring and Computing,* vol. 27, no. 5, pp. 567-568, 2013, doi: 10.1007/s10877-013-9470-5.

[17] H. R. v. Genderingen, M. Gevers, and W. W. M. Hack, "Intra-arterial pressure measurement in neonates: dynamic response requirements," *Physiological Measurement,* vol. 16, no. 1, pp. 55-61, 1995, doi: 10.1088/0967-3334/16/1/007.

[18] E. Dempsey and I. Seri, "Definition of Normal Blood Pressure Range: The Elusive Target," in *Hemodynamics and Cardiology: Neonatology Questions and Controversies*, I. Seri, M. Kluckow, and R. A. Polin Eds., 3 ed. Philadelphia, PA: Elsevier, Inc., 2019, ch. 3, pp. 47-64.

[19] R. M. Gardner, "System Concepts For Invasive Pressure Monitoring," in *Techniques and Procedures in Critical Care*, R. W. Taylor, J. M. Civetta, and R. R. Kirby Eds. Philadelphia, PA: Lippincott Inc Publishers, 1990, ch. 4, pp. 50-62.

[20] H. van Langen, P. Brienesse, K. Kopinga, and P. Wijn, "Dynamic response of a neonatal catheter-manometer system in situ," *Journal of clinical monitoring,* vol. 9, no. 5, pp. 335-40, 1993, doi: 10.1007/bf01618675.

[21] B. Lambermont *et al.*, "Correction of pressure waveforms recorded by fluid-filled catheter recording systems: A new method using a transfer equation," *Acta Anaesthesiologica Scandinavica,* vol. 42, no. 6, pp. 717-720, 1998, doi: 10.1111/j.1399-6576.1998.tb05307.x.

[22] L. Hazeleger, "Validity and reconstruction of the intra-arterial blood pressure waveform measured with a catheter-manometer system in critically ill neonates," Master of Science, Radboudumc Amalia Children's Hospital, Nijmegen, The Netherlands, University of Twente, Enschede, The Netherlands, 2022.

[23] M. H. Hines, "Neonatal cardiovascular physiology," *Seminars in Pediatric Surgery,* vol. 22, no. 4, pp. 174-178, 2013, doi: 10.1053/j.sempedsurg.2013.10.004.

[24] R. I. Clyman, "Mechanisms Regulating the Ductus Arteriosus," *Neonatology,* vol. 89, no. 4, pp. 330-335, 2006, doi: 10.1159/000092870.

[25] Y. Singh, A. C. Katheria, and F. Vora, "Advances in Diagnosis and Management of Hemodynamic Instability in Neonatal Shock," *Frontiers in pediatrics,* vol. 6, pp. 2-2, 2018, doi: 10.3389/fped.2018.00002.

[26] T.-W. Wu, T. Azhibekov, and I. Seri, "Transitional Hemodynamics in Preterm Neonates: Clinical Relevance," *Pediatrics & Neonatology,* vol. 57, no. 1, pp. 7-18, 2016, doi: 10.1016/j.pedneo.2015.07.002.

[27] R. E. Giesinger, L. J. Bailey, P. Deshpande, and P. J. McNamara, "Hypoxic-Ischemic Encephalopathy and Therapeutic Hypothermia: The Hemodynamic Perspective," *The Journal of Pediatrics,* vol. 180, pp. 22-30.e2, 2017, doi: 10.1016/j.jpeds.2016.09.009.

[28] J. M. Dionne *et al.*, "Method of Blood Pressure Measurement in Neonates and Infants: A Systematic Review and Analysis," *The Journal of Pediatrics,* vol. 221, pp. 23-31.e5, 2020, doi: 10.1016/j.jpeds.2020.02.072.

[29] B. E. Westerhof, M. J. C. van Gemert, and J. P. van den Wijngaard, "Pressure and Flow Relations in the Systemic Arterial Tree Throughout Development From Newborn to Adult," *Frontiers in Pediatrics,* vol. 8, 2020, doi: 10.3389/fped.2020.00251.

[30] M. F. O'Rourke, A. Pauca, and X.-J. Jiang, "Pulse wave analysis," *British Journal of Clinical Pharmacology,* vol. 51, no. 6, pp. 507-522, 2001, doi: 10.1046/j.0306-5251.2001.01400.x.

[31] M. Gevers, H. R. Van Genderingen, K. V. Der Mooren, H. N. Lafeber, W. W. M. Hack, and N. Westerhof, "Bisferiens Peaks in the Radial Artery Pressure Wave in Newborn Infants: A Sign of Patent Ductus Arteriosus," *Pediatric Research,* vol. 37, no. 6, pp. 800-805, 1995, doi: 10.1203/00006450-199506000-00021.

[32] S. A. Esper and M. R. Pinsky, "Arterial waveform analysis," *Best Practice & Research Clinical Anaesthesiology,* vol. 28, no. 4, pp. 363-380, 2014, doi: 10.1016/j.bpa.2014.08.002.

[33] M. Nirmalan and P. M. Dark, "Broader applications of arterial pressure wave form analysis," *Continuing Education in Anaesthesia Critical Care & Pain,* vol. 14, no. 6, pp. 285-290, 2014, doi: 10.1093/bjaceaccp/mkt078.

[34] J. P. Murgo, N. Westerhof, J. P. Giolma, and S. A. Altobelli, "Aortic input impedance in normal man: relationship to pressure wave forms," *Circulation,* vol. 62, no. 1, pp. 105-116, 1980, doi: 10.1161/01.CIR.62.1.105.

[35] B. E. Westerhof and N. Westerhof, "Magnitude and return time of the reflected wave: the effects of large artery stiffness and aortic geometry," *Journal of Hypertension,* vol. 30, no. 5, 2012, doi: 10.1097/HJH.0b013e3283524932.

[36] T. Murakami *et al.*, "Aortic pressure wave reflection in children," *Hypertension Research,* vol. 33, no. 3, pp. 225-228, 2010, doi: 10.1038/hr.2009.218.

[37] M. Calamandrei, L. Mirabile, S. Muschetta, G. F. Gensini, L. De Simone, and S. M. Romano, "Assessment of cardiac output in children: A comparison between the pressure recording analytical method and Doppler echocardiography*," *Pediatric Critical Care Medicine,* vol. 9, no. 3, 2008, doi: 10.1097/PCC.0b013e31816c7151.

[38] R. Saxena, A. Durward, N. K. Puppala, I. A. Murdoch, and S. M. Tibby, "Pressure recording analytical method for measuring cardiac output in critically ill children: a validation study," *British Journal of Anaesthesia,* vol. 110, no. 3, pp. 425-431, 2013, doi: 10.1093/bja/aes420.

[39] R. H. Thiele and M. E. Durieux, "Arterial Waveform Analysis for the Anesthesiologist: Past, Present, and Future Concepts," *Anesthesia & Analgesia,* vol. 113, no. 4, 2011, doi: 10.1213/ANE.0b013e31822773ec.

[40] M. I. Monge Garcia *et al.*, "Performance comparison of ventricular and arterial dP/dtmax for assessing left ventricular systolic function during different experimental loading and contractile conditions," *Critical Care,* vol. 22, no. 1, p. 325, 2018, doi: 10.1186/s13054-018-2260-1.

[41] M. T. Politi *et al.*, "The dicrotic notch analyzed by a numerical model," *Computers in Biology and Medicine,* vol. 72, pp. 54-64, 2016, doi: 10.1016/j.compbiomed.2016.03.005.

[42] C. Kotidis, D. Wertheim, M. Weindling, H. Rabe, and M. A. Turner, "Assessing patent ductus arteriosus in preterm infants from standard neonatal intensive care monitoring," *European Journal of Pediatrics,* vol. 181, no. 3, pp. 1117-1124, 2022, doi: 10.1007/s00431-021-04311-9.

[43] R. A. Peura, "Blood pressure and sound," in *Medical instrumentation: application and design*, J. G. Webster Ed., 4 ed.: John Wiley & Sons, Inc., 2010, ch. 7, pp. 293-337.

[44] *Configuration Guide IntelliVue Patient Monitor (MX80, MP2/5/20/30/40/50/60/70/80/90, MP5T/MP5SC/X2)*, Philips Medizin Systeme Boeblingen GmbH, 2010. [Online]. Available: https://www.documents.philips.com/assets/Instruction%20for%20Use/20220223/51414b09bd404c5ba256ae4501365f69.pdf?feed=ifu_docs_feed. Accessed: 15-11-2022.

[45] R. A. Peura and J. G. Webster, "Basic sensors and principles," in *Medical instrumentation: application and design*, J. G. Webster Ed., 4 ed.: John Wiley & Sons, Inc, 2010, ch. 2, pp. 45-90.

[46] W. W. M. Hack, N. Westerhof, T. Leenhoven, and A. Okken, "Accurate measurement of intraarterial pressure through radial artery catheters in neonates," *Journal of Clinical Monitoring,* vol. 6, no. 3, pp. 211-216, 1990, doi: 10.1007/BF02832149.

[47] H. Oh, S. H. Choe, Y. J. Kim, H.-K. Yoon, H.-C. Lee, and H.-P. Park, "Intraarterial catheter diameter and dynamic response of arterial pressure monitoring system: a randomized controlled trial," *Journal of Clinical Monitoring and Computing,* vol. 36, no. 2, pp. 387-395, 2022, doi: 10.1007/s10877-021-00663-7.

[48] S. Devasahayam, N. Gangadharan, C. Surekha, B. Baskaran, F. A. Mukadam, and S. Subramani, "Intra-arterial blood pressure measurement: sources of error and solutions," *Medical & Biological Engineering & Computing,* vol. 60, no. 4, pp. 1123-1138, 2022, doi: 10.1007/s11517-022-02509-z.

[49] B. Kleinman, S. Powell, and R. M. Gardner, "Equivalence of fast flush and square wave testing of blood pressure monitoring systems," *Journal of Clinical Monitoring,* vol. 12, no. 2, pp. 149-154, 1996, doi: 10.1007/BF02078135.

[50] B. Kleinman, S. Powell, P. Kumar, and Reed M. Gardner, "The Fast Flush Test Measures the Dynamic Response of the Entire Blood Pressure Monitoring System," *Anesthesiology,* vol. 77, no. 6, pp. 1215-1220, 1992, doi: 10.1097/00000542-199212000-00024.

[51] E. Billiet and F. Colardyn, "Hazardous Information from Bedside Fast-Flush Device Test for Fluid-Filled Pressure Monitoring Systems," *Angiology,* vol. 43, no. 12, pp. 988-995, 1992, doi: 10.1177/000331979204301205.

[52] D. T. Soule and D. J. Powner, "Air entrapment in pressure monitoring lines," *Critical Care Medicine,* vol. 12, no. 6, 1984.

[53] L. Bocchi and S. Romagnoli, "Resonance artefacts in modern pressure monitoring systems," *Journal of Clinical Monitoring and Computing,* vol. 30, no. 5, pp. 707-714, 2016, doi: 10.1007/s10877-015-9760-1.

[54] L. T. Hersh, B. Friedman, W. Luczyk, and J. Sesing, "Evaluation of filtering methods for acquiring radial intra-artery blood pressure waveforms," *Journal of Clinical Monitoring and Computing,* vol. 29, no. 5, pp. 659-669, 2015, doi: 10.1007/s10877-014-9649-4.

[55] S. Devasahayam, N. Gangadharan, C. Surekha, B. Baskaran, F. A. Mukadam, and S. Subramani, "Intra-arterial blood pressure measurement: sources of error and solutions," *Medical and Biological Engineering and Computing,* vol. 60, no. 4, pp. 1123-1138, 2022, doi: 10.1007/s11517-022-02509-z.

[56] S. Romagnoli, F. Franchi, Z. Ricci, S. Scolletta, and D. Payen, "The Pressure Recording Analytical Method (PRAM): Technical Concepts and Literature Review," *Journal of Cardiothoracic and Vascular Anesthesia,* vol. 31, no. 4, pp. 1460-1470, 2017, doi: 10.1053/j.jvca.2016.09.004.

[57] S. Romagnoli *et al.*, "Dynamic response of liquid-filled catheter systems for measurement of blood pressure: precision of measurements and reliability of the Pressure Recording Analytical Method with different disposable systems," *Journal of Critical Care,* vol. 26, no. 4, pp. 415-422, 2011, doi: 10.1016/j.jcrc.2010.08.010.

[58] R. Melamed, K. Johnson, B. Pothen, M. D. Sprenkle, and P. J. Johnson, "Invasive blood pressure monitoring systems in the ICU: influence of the blood-conserving device on the dynamic response characteristics and agreement with noninvasive measurements," *Blood Pressure Monitoring,* vol. 17, no. 5, 2012, doi: 10.1097/MBP.0b013e328356e1c7.

[59] B. Kleinman, K. Frey, and R. Stevens, "The Fast Flush Test – Is the Clinical Comparison Equivalent to its In Vitro Simulation?," *Journal of Clinical Monitoring and Computing,* vol. 14, no. 7, pp. 485-489, 1998, doi: 10.1023/A:1009987329163.

[60] M. P. Mulder, M. Broomé, D. W. Donker, and Berend E. Westerhof, "Distinct morphologies of arterial waveforms reveal preload-, contractility-, and afterload-deficient hemodynamic instability: An in silico simulation study," *Physiological Reports,* vol. 10, no. 7, p. e15242, 2022, doi: 10.14814/phy2.15242.

[61] M. Gevers, W. W. Hack, E. F. Ree, H. N. Lafeber, and N. Westerhof, "Arterial blood pressure wave forms in radial and posterior tibial arteries in critically ill newborn infants," *J Dev Physiol,* vol. 19, no. 4, pp. 179-185, 1993.

[62] T. L. Gomella, M. D. Cunningham, F. G. Eyal, and D. J. Tuttle, "Arterial Access: Umbilical Artery Catheterization," in *Neonatology: Management, Procedures, On-Call Problems, Diseases, and Drugs*, 7 ed. New York, NY: McGraw-Hill Education, 2013.

[63] S. Scolletta, S. M. Romano, B. Biagioli, G. Capannini, and P. Giomarelli, "Pressure recording analytical method (PRAM) for measurement of cardiac output during various haemodynamic states," *British Journal of Anaesthesia,* vol. 95, no. 2, pp. 159-165, 2005, doi: 10.1093/bja/aei154.

[64] C. J. Hartley, A. K. Reddy, and G. E. Taffet, "In-vitro evaluation of sensors and amplifiers to measure left ventricular pressure in mice," *2008 30th Annual International Conference of the IEEE Engineering in Medicine and Biology Society,* pp. 965-968, 2008, doi: 10.1109/IEMBS.2008.4649315.

[65] M. Gevers, H. R. van Genderingen, H. N. Lafeber, and W. W. Hack, "Radial artery blood pressure measurement in neonates: an accurate and convenient technique in clinical practice," *Journal of perinatal medicine,* vol. 23, no. 6, pp. 467–475, 1995, doi: 10.1515/jpme.1995.23.6.467.

[66] H. R. van Genderingen, M. Gevers, and W. W. M. Hack, "Prevention of air introduction in catheter-manometer systems for accurate neonatal blood pressure measurement: An in vitro study," *Journal of Clinical Monitoring,* vol. 10, no. 1, pp. 35-38, 1994, doi: 10.1007/BF01651464.

[67] B. Kleinman and S. Powell, "Dynamic response of the rose damping device," *Journal of Clinical Monitoring,* vol. 5, no. 2, pp. 111-115, 1989, doi: 10.1007/BF01617884.

[68] D. T. Johnson, S. Fournier, R. L. Kirkeeide, B. De Bruyne, K. L. Gould, and N. P. Johnson, "Phasic pressure measurements for coronary and valvular interventions using fluid-filled catheters: Errors, automated correction, and clinical implications," *Catheterization and Cardiovascular Interventions,* vol. 96, no. 3, pp. E268-E277, 2020, doi: 10.1002/ccd.28780.

[69] X. Quan *et al.*, "Advances in Non-Invasive Blood Pressure Monitoring," *Sensors,* vol. 21, no. 13, 2021, doi: 10.3390/s21134273.

[70] S. Tibby, "Transpulmonary thermodilution: Finally, a gold standard for pediatric cardiac output measurement*," *Pediatric Critical Care Medicine,* vol. 9, no. 3, 2008, doi: 10.1097/PCC.0b013e318172ea56.

[71] J. Cauwenberge *et al.*, "Assessing the Performance of Ultrafast Vector Flow Imaging in the Neonatal Heart via Multiphysics Modeling and In Vitro Experiments," *IEEE Transactions on Ultrasonics, Ferroelectrics, and Frequency Control,* vol. 63, pp. 1-1, 2016, doi: 10.1109/TUFFC.2016.2596804.

[72] Y. N. Elsayed, R. Amer, and M. M. Seshia, "The impact of integrated evaluation of hemodynamics using targeted neonatal echocardiography with indices of tissue oxygenation: a new approach," *Journal of Perinatology,* vol. 37, no. 5, pp. 527-535, 2017, doi: 10.1038/jp.2016.257.

[73] H. A. d. A. Serra and N. Paulino, "Butterworth Filtering Transfer Function," in *Design of Switched-Capacitor Filter Circuits using Low Gain Amplifiers*: Springer International Publishing, 2015, pp. 83-92.

Appendix

A Derivation of the Equations for Natural Frequency and Damping Coefficient

Based on Figure 2.3 and Kirchhoff's voltage law, the output signal $O(t)$, analogous to the pressure sensed at the diaphragm, is given by:

$$O(t) = I(t) - L_c \frac{dQ(t)}{dt} - R_c Q(t) = I(t) - L_c C_d \frac{dO^2(t)}{dt^2} - R_c C_d \frac{dO(t)}{dt}, \quad \text{(Eq. A.1)}$$

with $I(t)$ the input signal, analogous to the applied pressure, $Q(t)$ the flow of liquid through the catheter, L_c the catheter liquid inertia, R_c the catheter liquid resistance and C_d the sensor diaphragm compliance. Rewriting gives:

$$\frac{dO^2(t)}{dt^2} + \frac{R_c}{L_c}\frac{dO(t)}{dt} + \frac{1}{L_c C_d} O(t) = \frac{1}{L_c C_d} I(t). \quad \text{(Eq. A.2)}$$

Comparing this to Equation 2.4, the following equations can be derived:

$$\omega_n{}^2 = \frac{1}{L_c C_d}, \quad \text{(Eq. A.3)}$$

and

$$2\omega_n \zeta = \frac{R_c}{L_c}, \quad \text{(Eq. A.4)}$$

with ω_n the natural angular frequency and ζ the damping coefficient. Rewriting and substituting Equations 2.1, 2.2 and 2.3 results in:

$$\omega_n = \sqrt{\frac{1}{L_c C_d}} = \sqrt{\frac{\pi r^2 K}{\rho L}} = r\sqrt{\frac{\pi K}{\rho L}}, \quad \text{(Eq. A.5)}$$

and

$$\zeta = \frac{R_c}{L_c}\frac{1}{2\omega_n} = \frac{8\eta L}{\pi r^4}\frac{\pi r^2}{\rho L}\frac{1}{2r}\sqrt{\frac{\rho L}{\pi K}} = \frac{4\eta}{r^3}\sqrt{\frac{L}{\pi \rho K}}, \quad \text{(Eq. A.6)}$$

where L and r are respectively the length and radius of the catheter, ρ is the fluid density, and η is the fluid viscosity. Finally, for the natural frequency (f_n) it holds that:

$$f_n = \frac{\omega_n}{2\pi} = \frac{r}{2\pi}\sqrt{\frac{\pi K}{\rho L}} = \frac{r}{2}\sqrt{\frac{K}{\pi \rho L}}. \quad \text{(Eq. A.7)}$$

B Derivation of the Step and Impulse Responses of the Monitoring System

The arterial blood pressure monitoring system consists of a liquid-filled CMS and monitor low pass filter. The CMS can be modelled as a second-order dynamic system according to the following equation:

$$\frac{d^2O(t)}{dt^2} + 2\omega_n\zeta\frac{dO(t)}{dt} + \omega_n^2 O(t) = \omega_n^2 I(t), \quad \text{(Eq. B.1)}$$

with $I(t)$ the input signal, analogous to the applied pressure, $O(t)$ the output signal, analogous the pressure at the diaphragm, ω_n the natural frequency in rad/s, and ζ the damping coefficient. The corresponding transfer function is given by:

$$H_{CMS}(s) = \frac{\omega_n^2}{s^2 + 2\omega_n\zeta s + \omega_n^2}, \quad \text{(Eq. B.2)}$$

with s the Laplace operator. The monitor low pass filter is assumed to be a second-order Butterworth filter, with the following transfer function [73]:

$$H_{butterworth}(s) = \frac{\omega_c^2}{s^2 + \sqrt{2}\omega_c s + \omega_c^2}, \quad \text{(Eq. B.3)}$$

with ω_c the cut-off frequency in rad/s. The transfer function of the total monitoring system is given by the multiplication of Equations B.2 and B.3:

$$H_{total}(s) = \frac{\omega_n^2}{s^2 + 2\omega_n\zeta s + \omega_n^2} \cdot \frac{\omega_c^2}{s^2 + \sqrt{2}\omega_c s + \omega_c^2} = \quad \text{(Eq. B.4)}$$

$$= \frac{\omega_n^2 \cdot \omega_c^2}{\left(s + \omega_n\zeta + \omega_n j\sqrt{1-\zeta^2}\right)\cdot\left(s + \omega_n\zeta - \omega_n j\sqrt{1-\zeta^2}\right)\cdot\left(s + \omega_c\frac{\sqrt{2}}{2} + \omega_c j\frac{1}{\sqrt{2}}\right)\cdot\left(s + \omega_c\frac{\sqrt{2}}{2} - \omega_c j\frac{1}{\sqrt{}}\right.}$$

where $j = \sqrt{-1}$ and $0 \leq \zeta < 1$, since the system is assumed to be underdamped.

Partial fraction expansion gives:

$$H_{total}(s) = \frac{c_1}{s + \omega_n\zeta + \omega_n j\sqrt{1-\zeta^2}} + \frac{c_2}{s + \omega_n\zeta - \omega_n j\sqrt{1-\zeta^2}} + \frac{c_3}{s + \omega_c\frac{\sqrt{2}}{2} + \omega_c j\frac{1}{\sqrt{2}}} + \frac{c_4}{s + \omega_c\frac{\sqrt{2}}{2} - \omega_c j\frac{1}{\sqrt{2}}}$$

The homogeneous solution of this equation is:

$$\begin{aligned} y_h(t) = {} & c_1 \cdot e^{-(\omega_n\zeta + \omega_n j\sqrt{1-\zeta^2})t} + c_2 \cdot e^{-(\omega_n\zeta - \omega_n j\sqrt{1-\zeta^2})t} + c_3 \cdot e^{-\left(\omega_c\frac{\sqrt{2}}{2} + \omega_c j\frac{1}{\sqrt{2}}\right)t} \\ & + c_4 \cdot e^{-\left(\omega_c\frac{\sqrt{2}}{2} - \omega_c j\frac{1}{\sqrt{2}}\right)t} \\ = {} & e^{-\omega_n\zeta t}\left(c_1 \cdot e^{-\omega_n j\sqrt{1-\zeta^2}t} + c_2 \cdot e^{\omega_n j\sqrt{1-\zeta^2}t}\right) \\ & + e^{-\omega_c\frac{\sqrt{2}}{2}t}\left(c_3 \cdot e^{-\omega_c j\frac{1}{\sqrt{2}}t} + c_4 \cdot e^{\omega_c j\frac{1}{\sqrt{2}}t}\right) \end{aligned} \quad \text{(Eq. B.5)}$$

Substituting Euler's equation and removing complex terms gives:

$$y_h(t) = e^{-\omega_n\zeta t}(c_1 + c_2)\cos\left(\omega_n\sqrt{1-\zeta^2}t\right) + e^{-\omega_c\frac{\sqrt{2}}{2}t}(c_3 + c_4)\cos\left(\omega_c\frac{1}{\sqrt{2}}t\right)$$

Using $\omega_n = 2\pi f_n$ and $\omega_c = 2\pi f_c$, with f_n the natural frequency of the CMS in Hz and f_c the cut-off frequency of the Butterworth filter in Hz, the following equation holds for the step and impulse responses of the monitoring system with different initial and final conditions:

$$P(t) = A \cdot e^{-2\pi f_n\zeta t} \cdot \sin\left(2\pi f_n \cdot \sqrt{1-\zeta^2} \cdot t + B\right) + C \cdot e^{-2\pi f_c\frac{\sqrt{2}}{2}t} \cdot \sin\left(2\pi f_c \cdot \frac{1}{\sqrt{2}} \cdot t + D\right) + E, \quad \text{(Eq. B.6)}$$

where $P(t)$ is the measured response in mmHg and A (in mmHg), B, C (in mmHg), D and E (in mmHg) are constants.

C Calculation of Arterial Blood Pressure Waveform Parameters

For the calculation of ABPW parameters, first the following landmarks are detected:

1. Wave onset:
    a. First, the peak in the first derivative of the ABPW is detected.
    b. Then, searching backward from this peak, the first zero-crossing prior to this peak is defined as the wave onset.
2. Systolic peak: the maximum of the ABPW.
3. Dicrotic notch:
    a. First, a search window is defined between the maximal negative slope of the systolic downstroke and two-thirds of the wave period.
    b. Secondly, if there is a local minimum of the ABPW within this search window, this is the dicrotic notch. If no local minima are found, a local maximum of the first derivative of the ABPW is detected as the dicrotic notch. In case this is neither found, the local maximum in the second derivative of the ABPW is chosen as the dicrotic notch.

After these landmarks are detected, the parameters are calculated as follow:

1. Mean pressure: the mean value of the ABPW between the two wave onsets.
2. Systolic pressure: the pressure at the systolic peak.
3. Diastolic pressure: the pressure at the first wave onset.
4. Pulse pressure: systolic pressure minus diastolic pressure.
5. Dicrotic notch pressure: the pressure at the dicrotic notch.
6. Maximal slope of the systolic upstroke: the maximum of the first derivative of the ABPW.
7. Area under the curve: the absolute area under the ABPW between the two wave onsets.
8. Systolic area under the curve: the absolute area under the ABPW between the first wave onset and the dicrotic notch.